2014

Synthesis and Evaluation of a Series of Novel Isoprenylated Coumarins as Potential Anti-Pancreatic Cancer Agents

Katherine Eyring
keyring@wellesley.edu

Synthesis and Evaluation of a Series of Novel Isoprenylated Coumarins as Potential Anti-Pancreatic Cancer Agents

Katie Eyring
Advisor: Dora Carrico-Moniz

Neuroscience Program

A Thesis Submitted in Partial Fulfillment of the Requirement for the Bachelor of Arts Degree with Honors in Neuroscience at Wellesley College

Acknowledgements

I could not have completed this thesis project alone. I have received unending support and guidance from a number of individuals throughout and I would like to acknowledge them here.

Professor Carrico Moniz, thank you for your patience and guidance. Thanks to you, I have learned what it means to do good science. Your optimism and encouragement in the face of disappointment is inspiring. As I go off to graduate school, I feel confident in myself because of you.

Kellen and Frieda, it is such a pleasure to work with the two of you. You both make weekend and late-night work fun!

Maria and Alyssa, thank you for your instruction and advice. You laid the groundwork for this study—it wouldn't have been possible without you.

Professors Webb and Beltz, thank you for all your input and guidance during the evolution of this project. It is all the better for it.

Dr. V, I know you always have my best interest in mind. Thank you for always checking in on me.

Christine Chun and other members of the DCM lab, your work has greatly contributed to the success of this project. I can only hope to support you in the same way you've supported me.

Jordan, Greg and Ben, thank you for your comments and patience.

Camylle, thank you for always being available for me to bounce ideas off of…even in the middle of the night.

Table of Contents

Abstract

Pancreatic cancer is an insidious and aggressive form of cancer, with a global mortality rate of nearly 98%. Recent therapeutic endeavors have sought natural products with intrinsic cytotoxicity against pancreatic cancer cell lines, including a series of coumarin derivatives with pronounced bioactivity against pancreatic adenocarcinoma cell lines. Structural variants of one such natural product, *Angelmarin*, provide insight into what structural elements are essential for specific bioactivity in nutrient-deprived conditions. The present study investigates the cytotoxicity of coumarin derivatives as a function of isoprenyl positioning, chain length, saturation and chirality. To this end, novel isoprenylated coumarin derivatives were synthesized and evaluated against PANC-1 cell lines under nutrient-deprived media (NDM) and nutrient-rich media (NRM) conditions. Coumarins isoprenylated at the C-4 position, with substituents of 10 and 15 carbons in length, exhibited LC_{50} values of 3.5 and 6 μM, respectively, against PANC-1 cells in nutrient-deprived conditions. Conversely, coumarins substituted with 10 carbon fully saturated or partially saturated chiral isoprenylated chains did not induce cell toxicity above 50% in NDM. These data implicate alkylation position as a primary structural determinant of coumarin-derived cytotoxicity; whereas, saturation and chirality appear inessential.

Introduction

Pancreatic cancer is an aggressive and insidious form of cancer with a global mortality rate of 98% [1]. While pancreatic cancer is not the most common form of cancer, it is the fourth most common cause of cancer-related deaths in the United States, in both men and women (Figure 1A, [2]). Typically, patients have less than a 5% survival rate within five years of their initial diagnosis (Figure 1B, [2]).

A **Pancreas and Cancer – Estimate Deaths**

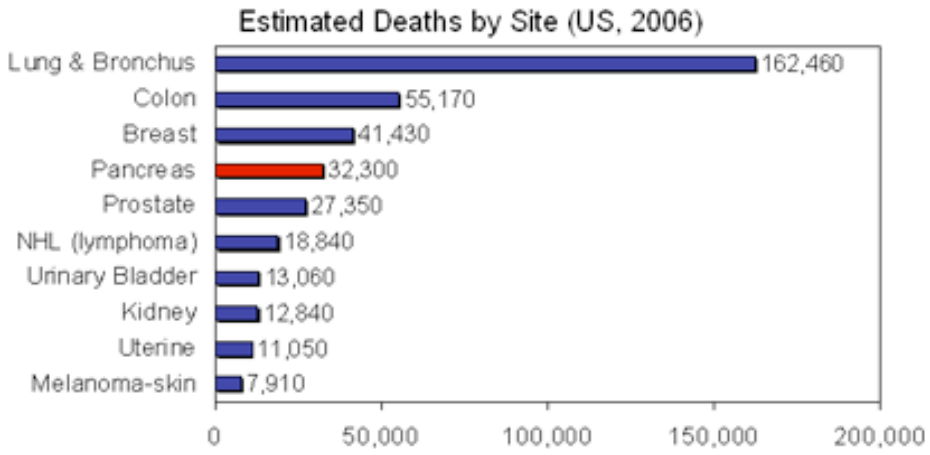

B **Pancreas and Cancer – Survival Rate**

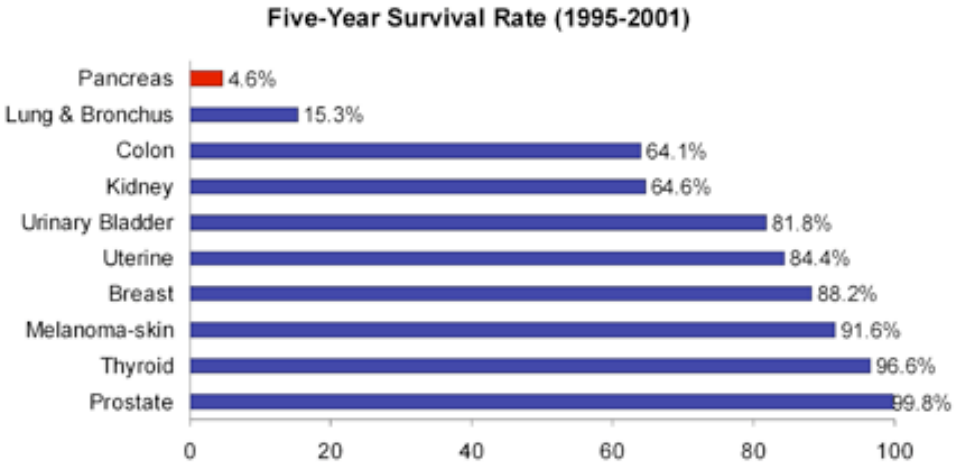

Figure 1. U.S deaths and survival rates attributed to different forms of cancer in 2006. Both men and women are considered in the data. (A) U.S deaths attributed to different forms of cancer, categorized by site of tumor origin. (B) U.S survival rates, within 5 years of diagnosis, attributed to different forms of cancer, categorized by site of tumor origin. Figures are reprinted from The Pancreas Center website, maintained by the Columbia University Department of Surgery [2].

The dismal survival rate associated with pancreatic cancer can be attributed to both the aggressive nature of the cancer, as well as its resistance to current therapies. In the

early stages of the disease most patients are asymptomatic, which often results in late-stage diagnosis and thus poor prognosis. Patients with the most common form of pancreatic cancer, pancreatic ductal adenocarcinoma (PDAC), experience a median survival time of just 6 months after diagnosis [3]. Pancreatic cancer cells are also remarkably resistant to conventional cancer therapies [4, 5]. Given that most patients are diagnosed in the advanced stages of the disease, surgical resection and radiation therapy are often implausible treatment options. Combinatorial treatment, in which multiple chemotherapeutic agents are used in concert, can improve median survival rate; though, at a taxing physical cost for the patient. To date, only 11 drugs have been approved for the treatment of pancreatic cancer, four of which are based on a compound (fluorouracil) that was described more than 50 years ago [6]. The absence of novel clinical treatments has prompted the search for natural products with intrinsic bioactivity against pancreatic cancer cells. More recent therapies boast innovative biochemical targets, such as tyrosine kinase inhibitors and nucleic acids that are required for cell division in an effort to differentially target the rapidly dividing cancer cell [6, 7]. Nevertheless, pancreatic cancer survival rates remain low. We propose that the notable resistance of pancreatic cancer cells to nutrient deprivation and hypoxia raises the possibility of a new drug target [8].

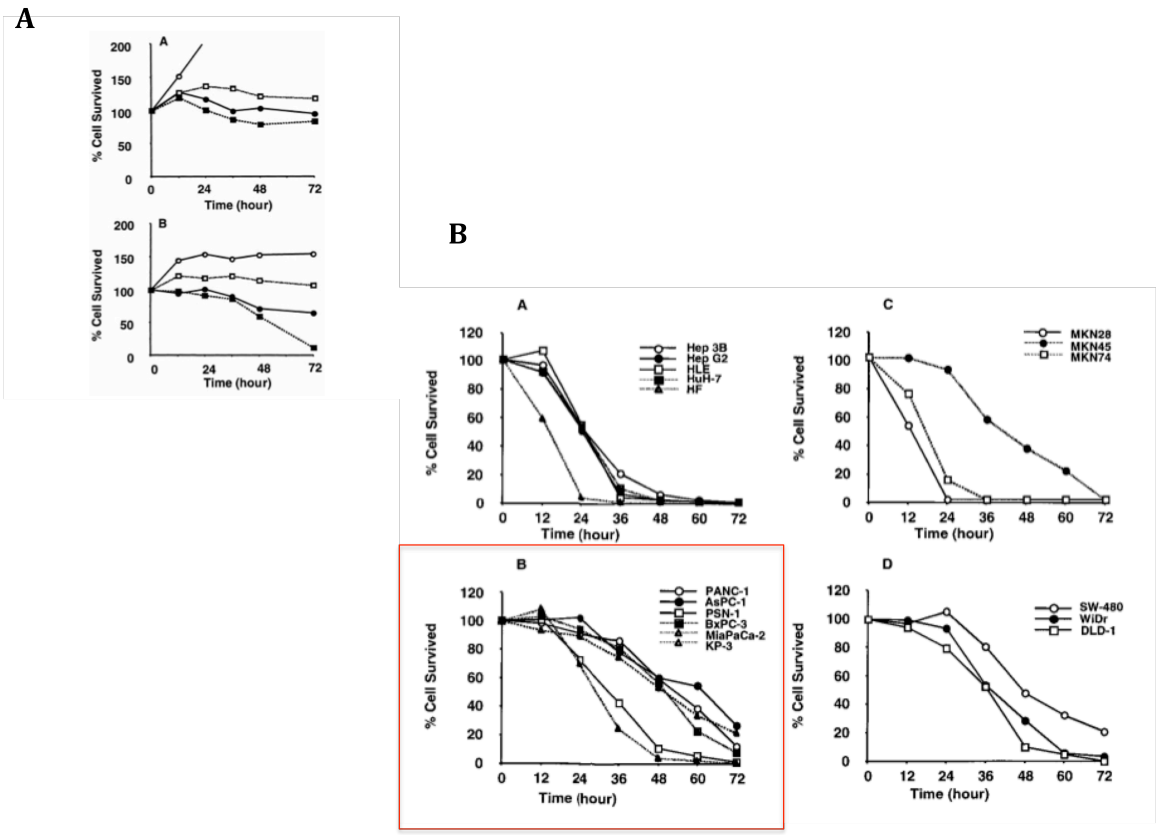

Figure 2. Austerity of pancreatic adencarcinoma (PANC-1) cell lines in nutrient-deprived conditions. (A) PANC-1 cell survival in the presence (A) and absence (B) of dialyzed fetal bovine serum, with the addition of (white circle) glucose and amino acids; (filled circle) glucose; (white square) amino acids; and (filled square) no nutrients. (B) Survival of various forms of cancer in the absence of nutrients or fetal bovine serum (A) liver cancer cell lines, (B) pancreatic cancer cell lines, (C) stomach cancer cell lines, and (D) colon cancer. Pancreatic cancer cell lines are highlighted in red. Figure adapted from Izuishi, et al [8].

In 2000, Izuishi and colleagues demonstrated the unique austerity of pancreatic cancer cells in nutrient deprived conditions (Figure 2, [8]). Pancreatic adenocarcinoma (PANC-1) cells remained essentially 100% viable when cultured in fetal bovine serum in the absence of supplemental amino acids and glucose (Figure 2Aa, [8]). In fact, appreciable numbers pancreatic cancer cells survived for up to three days without any form of nutrients (Figure 2, [8]). Significantly, when compared to other forms of cancer,

pancreatic cell lines are more tolerant of nutrient deprivation (Figure 2B, [8]). This austerity in nutrient deprived conditions is thought to underlie the unremitting nature of pancreatic tumors. As tumors grow, they become decreasingly innervated by blood vessels, and thus deprived of nutrients and oxygen. Nutrient deprivation and hypoxia, in turn, can lead to increased mutagenesis and genomic instability, increasing the incidence of cancerous growths [9]. As such, recent therapeutic endeavors have focused attention on natural products with intrinsic cytotoxicity against pancreatic cancer cell lines in nutrient deprived conditions.

Historically, natural products have been of considerable medicinal interest due to their high solubility and low toxicity when compared to synthetic compounds [10]. In the 1950's, the United States began investigating naturally occurring compounds with intrinsic bioactivities against cancerous malignancies. Such endeavors led to the discovery of Taxol, once the most widely prescribed chemotherapy drug in the world [11]. Ongoing global efforts have led to the discovery of numerous natural products that serve as lead compounds in the development of therapies for cancerous tumors. The discovery process begins with crude extracts being isolated from the roots or leaves of plants with traditional medicinal uses and tested against a diverse selection of cancer cell lines. Structures with promising bioactivities are then characterized and isolated to then serve as parent compounds in a series of structure activity relationship (SAR) studies. In SAR studies, slight structural variations are made on the parent compound to determine the moieties that contribute to cytotoxicity. The initial structure can then be modified to maximize activity and specificity against the drug target, before moving further down the drug development "pipeline".

Angelmarin (**1**), a natural product isolated from the root of the Japanese medicinal shrub *Angelica pubescens* in 2006, has exhibited specific and promising cytotoxicity against pancreatic cancer cell lines in nutrient deprived conditions (Figure 3, [12]).

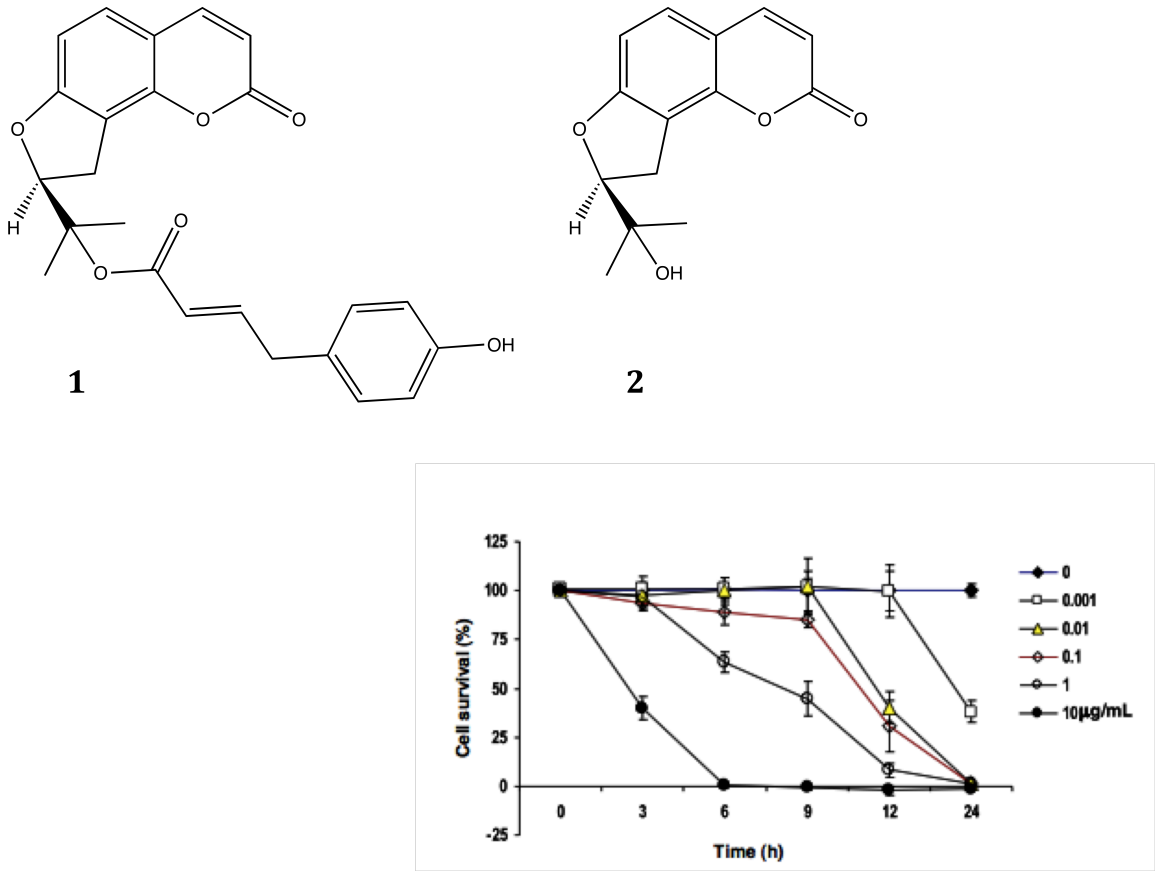

Figure 3. Angelmarin (**1**) and its bioactivity against PANC-1 cells in nutrient-deprived media (NDM). (A) The structure of Angelmarin **(1)** and one of its structural precursors **(2),** as determined by Awale and colleagues [12]. (B) Survival of PANC-1 cells in NDM at various concentrations. Both figures adapted from Awale, et al [12].

Within a six-hour incubation period, *Angelmarin* was found to kill 100% of pancreatic adenocarcinoma (PANC-1) at a concentration of just 10 µg/mL (Figure 3, [12]). Indeed, concentrations of 0.01 µg/mL were sufficient to kill all cancerous cells within 24 hours (Figure 3, [12]). Additionally, this bioactivity was specific to cancerous

cells under nutrient deprived conditions. Even at concentrations of 100 μg/mL, *Angelmarin* remained innocuous to normal cells [12]. It follows that something unique to the structure of *Angelmarin* results in the specific cytotoxicity against PANC-1 cells in nutrient deprived conditions, which has made it of significant interest to the medicinal chemistry community. Structurally, *Angelmarin* contains a coumarin backbone, substituted at the 7^{th} and 8^{th} positions by an alkylated furan. Interestingly, a structural precursor to *Angelmarin* (**2**) isolated from the *A. pubescens* plant did not exhibit the same unique bioactivity (Figure 3A, [12]). This discrepancy in activity suggests that preferential cytotoxicity against PANC-1 cells in nutrient deprived conditions may be imparted by *Angelmarin*'s hydrocarbon tail.

Coumarin-based natural products isolated from the *Ferula assa-foetida* plant (located predominantly in Iran, Afghanistan and mainland China), which has traditionally been used to treat whooping cough and diseases of the nervous system, have also demonstrated remarkable cytotoxicity against a variety of cancer cell lines [13, 14]. While numerous coumarins have been isolated from the *Ferula* genus, Lee et al. recently isolated a number of coumarin derivatives (**3, 4**) with pronounced antiviral and cytotoxic character (Figure 4, [13, 15]).

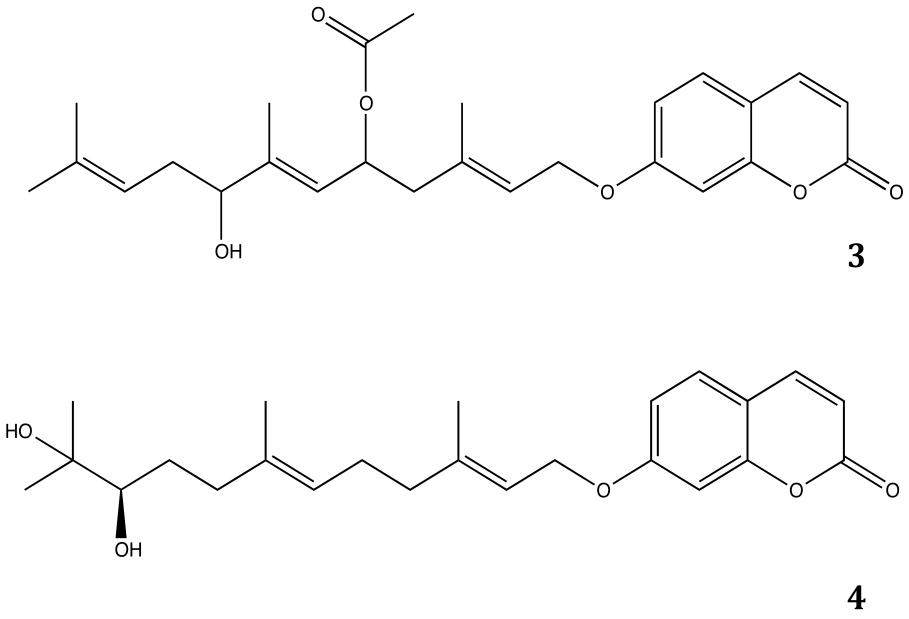

Figure 4. Sampling of coumarin derivatives isolated from *Ferula assa-foetida* by Lee and colleagues [13]. These examples contain a coumarin backbone, substituted at the C-7 position with hydrocarbon tails [13].

The majority of these compounds contain a coumarin scaffold that is substituted at the C-7 position by a farnesyl-derived moiety [13]. Again, it is likely that coumarin-derivative anti-viral and anti-tumoral activity is a consequence of the isoprenyl coumarin substituents; though, in-depth mechanistic studies have yet to be performed.

Another family of coumarins, isolated from the *Kayea assamica* flower, which is native to Myanmar, has demonstrated preferential cytotoxicity against PANC-1 cells in nutrient deprived conditions at concentrations of 1 μM [5]. Application of the compounds reported in this study can induce morphological changes in PANC-1 cells that are indicative of apoptosis. Interestingly, Win and colleagues proposed that an isoprenoid substituent at the C-8 position, in conjunction with a hydroxypropyl group at the C-4 position led to maximal observed cytotoxicity (**5**) [5].

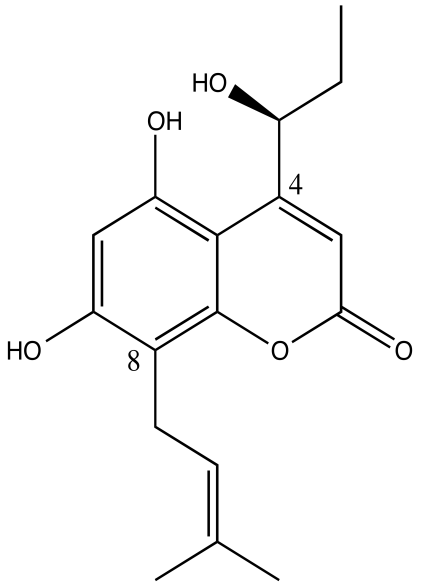

5

Figure 5. Substructure of coumarins isolated from *Kayea assamica* plant by Win and colleagues that exhibited most potent cytotoxicity against PANC-1 cells in nutrient deprived conditions.

Moreover, the addition of rigid structural groups at the C-4 and C-8 positions significantly decreased potency; whereas, the exchange of more flexible hydrocarbon groups such as geranyl and oxobutyl moieties at the C-6 and C-8 positions, in the presence of a hydroxypropyl group at C-4, retained PANC-1 cytotoxicity [5].

Previously, our laboratory explored the bioactivity of simplified structural coumarin intermediates against PANC-1 cells in work towards the total synthesis of *Angelmarin* (Figure 7).

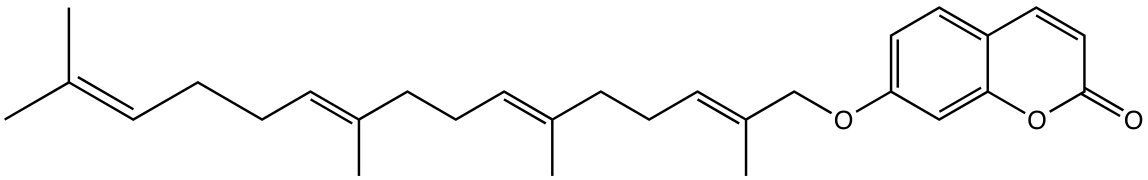

6

Figure 6. Coumarin derivative with potent bioactivity (LC_{50} = 6.25 μM) against PANC-1 cells in NDM. Compound synthesized by Devji, et al [16].

Remarkably, we found that several simple coumarin derivatives exhibited specific cytotoxicity against PANC-1 cells in nutrient-deprived conditions. Indeed, coumarins alkylated at the C-7 position were found to kill PANC-1 cells at micromolar concentrations (Figure 6,7; [16]).

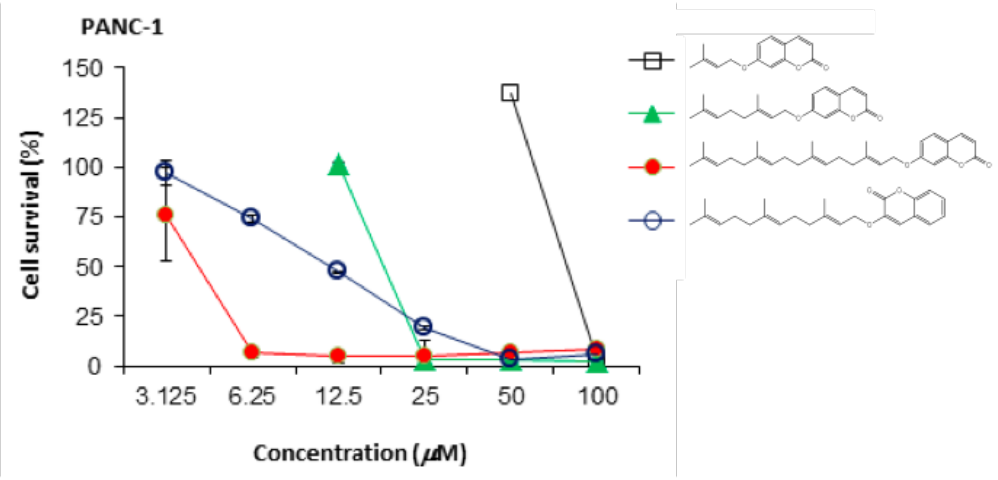

Figure 7. Cytotoxicity of a series of coumarin derivatives following 24 hour incubation with PANC-1 cells in nutrient-deprived media. Figure from [16].

The level of cytotoxicity was dependent on the identity of the substituted moiety. Specifically, the length of isoprenyl chains was directly correlated with increased

cytotoxicity against PANC-1 cells in nutrient deprived media [16]. Based on this prior work, the present study further investigates the cytotoxicity of coumarin derivatives against PANC-1 cells, and probes the underlying biological mechanisms of action of the coumarin-based compounds derived cytotoxicity.

Coumarins have represented a canonical class of natural products since the early 1800's [17]. They are of significant medicinal interest due to their wide range of biological activities. To date, coumarins have exhibited varied intrinsic bioactivities, including: antiviral, antibacterial, antiparasitic, anti-microbial, antioxidant, anticoagulant, antimicrobial and anticancer properties [17, 18]. Coumarins are also known to have anti-psychotic and anti-degenerative properties, as well as signaling capabilities at dopaminergic and serotinergic receptors, implicating a functional role for coumarins in the central nervous system [17]. Similar compounds are also known to reduce the accumulation of Aβ proteins in the cell and are in the clinical stage of development in the treatment of Alzheimer's disease (AD) [19]. This efficacy has been attributed to coumarin bioactivity against acetylcholinesterase (AChE) and beta-site amyloid precursor protein [APP] cleavage enzyme (BACE-1) [20]. AChE is an enzyme that breaks down acetylcholine, reducing the available acetylcholine in the synaptic cleft. AChE has also been implicated in the deposition of Aβ aggregates and can induce Aβ fibril formation. BACE-1 is an enzyme that is necessary for the production of the Aβ protein [20].

Structurally, coumarins are characterized by a bicyclic, conjugated ring system with a lactone moiety (Figure 8).

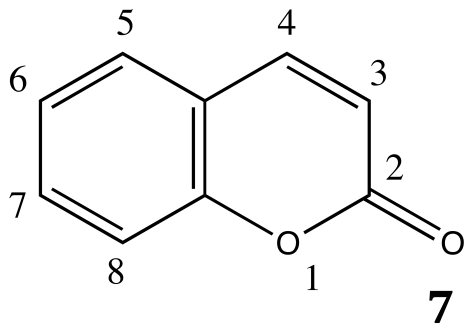

7

Figure 8. Basic coumarin chemical structure.

Coumarins can be further classified into four subgroups on the basis of their ring substituents: 1) simple coumarins, 2) furanocoumarins, 3) pyranocoumarins, and 4) bis/tri-coumarins [19]. Most naturally occurring coumarins are substituted at the 6, 7, or 8 positions [17].

Despite the robust and specific bioactivities of many coumarins, few have made it to the clinical stage of development. This discrepancy may be attributed to the limited synthetic and biological availability of most coumarins [18]. Coumarins have been isolated from numerous plant, fruit, bacterial and animal species [17]. However, natural resources are limited and the purification of coumarin derivatives is a time-consuming process often resulting in low yields. Few total syntheses for naturally occurring coumarin-containing compounds have been published, largely due to the numerous stereogenic centers present in these complex coumarin derivatives (for example, see **8**).

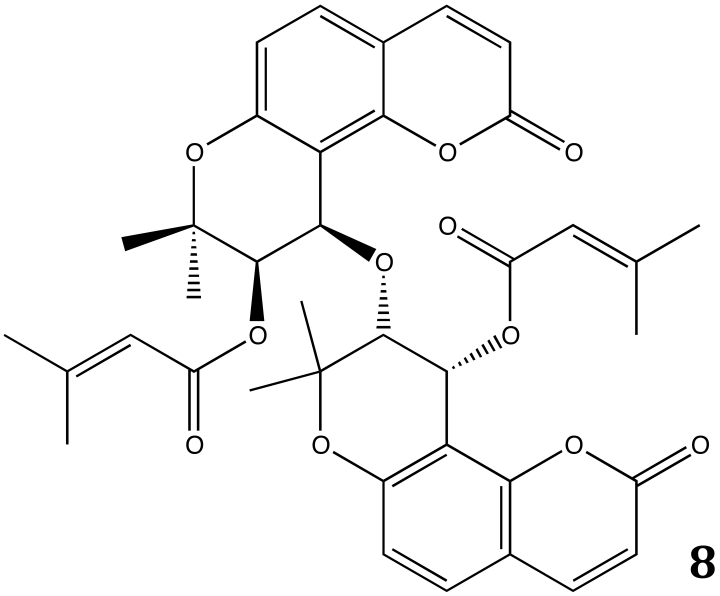

Figure 9. Natural product, **8**, was isolated from the aerial root of the *Angelica urumeinsis* plant and has exhibited antioxidative properties [21].

In fact, due to their structural complexity, some coumarins, like novobicin (**9)**, must be biosynthetically engineered from bacterial sources [22].

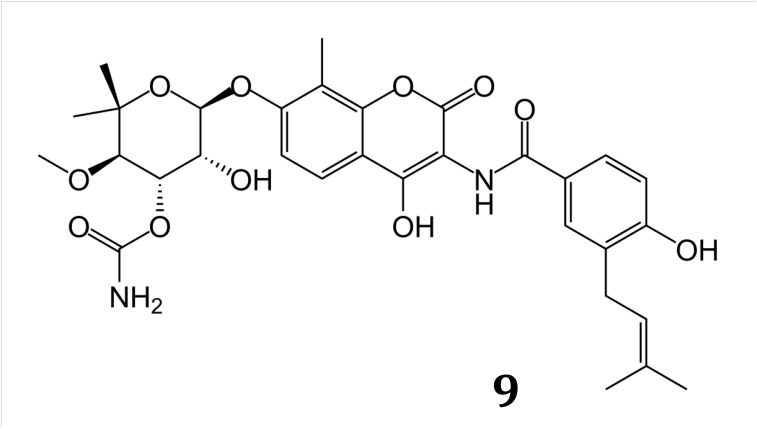

Figure 10. The antibiotic, Novobiocin (**9**).

Consequently, research efforts have focused predominantly on the most synthetically accessible sub-class of coumarins, simple coumarins.

Simple coumarins are characterized by the presence of hydroxy, alkoxy and alkyl substituents and will be the focus of the present investigation [17]. They can exhibit potent bioactivities in a variety of biological conditions [16, 17]. For instance, 4-hydroxycoumarin derivatives are known to possess more anti-coagulant activity than the globally produced anti-coagulant, Warfarin **(10).**

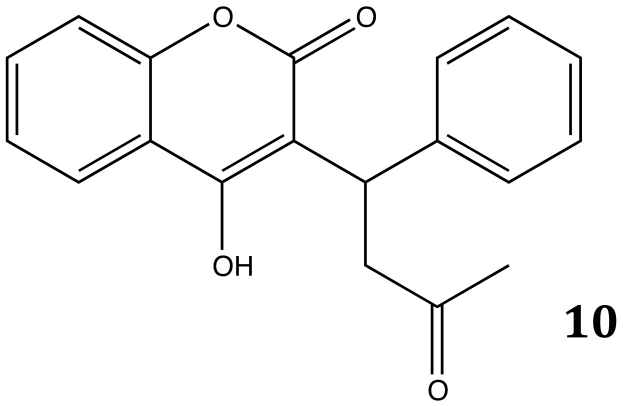

10

Figure 11. Structure of the anticoagulant, Warfarin (**10**).

A series of simple coumarin derivatives are known to inhibit the activity of HIV-1 protease (HIV-PR), which is necessary for the viral life cycle; the HIV-1 integrase enzyme that facilitates the assimilation of viral DNA in the host cell; and human papillomavirus (HPV-1) [17]. The unsubstituted coumarin scaffold itself has shown to have low anti-bacterial activity, while the addition of hydrocarbon chains significantly increases efficacy. Yet another simple coumarin derivative, a disubstituted coumarin, has shown activity against multi-drug resistant (MDR) strains of cancer **(11,** [19]).

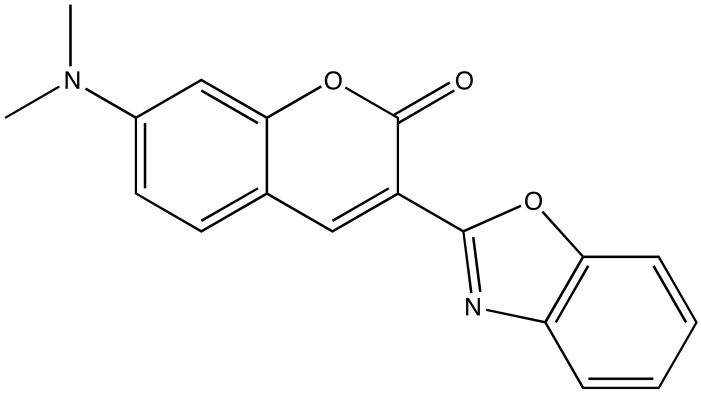

11

Figure 12. Structure of 7-Diethylamino-3(2`-benzoxazolyl)-coumarin (DBC). DBC is effective against multi-drug resistant (MDR) strains of various cancers [19].

Despite the relative structural simplicity of simple coumarins, they can exhibit diverse bioactivities. Coumarin substituents, and not the bicyclic lactone, are thought to be essential for bioactivity. For instance, anti-fungal and anti-bacterial activity has been attributed to free hydroxyl groups at the C-6 and C-7 positions, respectively; while, the antioxidant properties of coumarins are directly linked to the number of free hydroxyl groups [19, 23].

The broad spectrum of coumarin-derived anticancer bioactivity may be related to its anti-radical and anti-oxidative properties [19]. Oxygen and nitrogen based reactive species are present throughout the body and are the normal byproduct of mitochondrial function. However, unregulated free radicals can cause oxidative stress leading to DNA damage, carcinogenesis and widespread cellular malfunction. Increased levels of iron, and thus iron ion, can also produce an excess of hydrogen peroxide, which can then lead to radical species production. So, coumarins are thought to be effective preventative cancer therapies by reducing the concentrations of free radicals and oxidative species in the cell, minimizing further damage to the cell [19]. It follows that coumarins may also constitute effective preventative treatments by reducing oxidative damage prior to

cancerous growth. High anti-oxidative activity has been specifically attributed to coumarins with minimal electron-withdrawing substituents and maximal electron density distribution, via resonance structures [19].

There are many naturally occurring anti-oxidative compounds, including vitamins A and E, whose activity could be supplemented by coumarin-based treatments [19]. Moreover, vitamins A and E (**12)** are structurally similar to isoprenylated coumarins, perhaps implicating isoprenyl chains in antioxidative properties [24, 25].

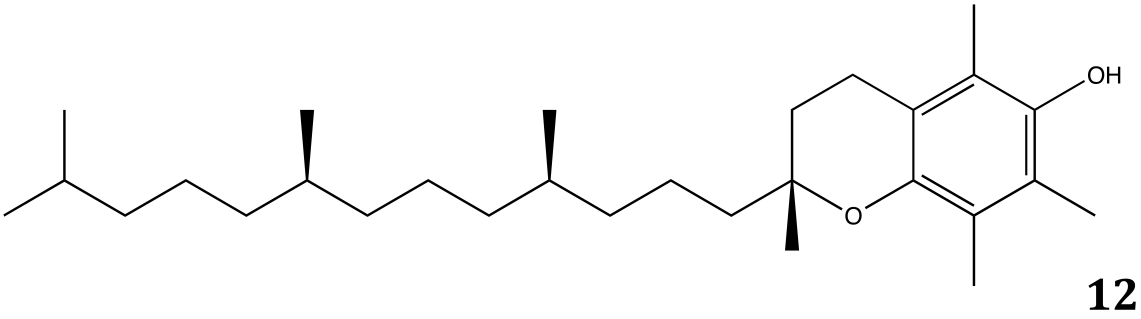

12

Figure 13. Chemical structure of vitamin E. Figure taken from [25].

These anti-oxidative capabilities are also thought to reduce cellular oxidative stress in the presence of Aβ aggregates in Alzheimer's disease (AD) and have motivated additional clinical trials of coumarin derivatives for Alzheimer's patients [19, 20]. In fact, the natural product Umbelliferone **(13)** reduces free radical levels in wild-type cells by up to 70-80% [26].

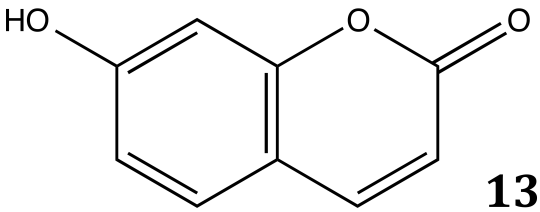

13

Figure 14. Chemical structure of Umbelliferone (**13**).

Coumarin derivatives isolated from the *Torpedo californica* plant have also exhibited inhibitory AChE activity in a reversible manner, sparking interest in the natural products as potential anti-AD agents. Ensaculain 1, **14**, a structural analog of the coumarin derivatives from the *T. californica* plant is currently in clinical trials for AD therapy [27].

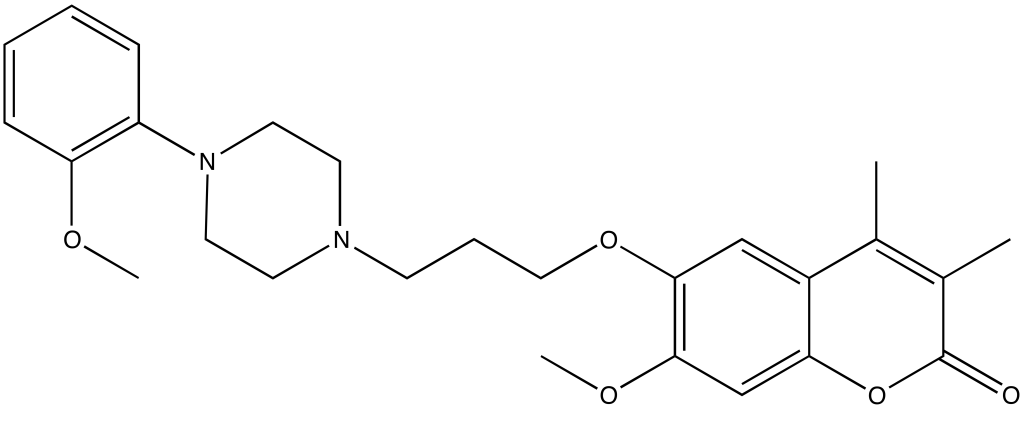

14

Figure 15. Chemical structure of Ensaculin (**14**).

Lipophilicity has been proposed as a critical determinant of coumarin-derived antioxidant activity and cytotoxicity [19, 24]. Each compound's lipophilicity is directly related to the length of its hydrocarbon substituents, providing a potential mechanism for the direct relationship between isoprenyl chain length and cytotoxicity [16]. Longer

carbon chains produce higher lipophilicities, thereby facilitating membrane integration. However, it remains unclear whether coumarins act within the cell or at the membrane surface. Recent work has suggested that some coumarin derivatives may, indeed, cross the cell membrane and act at the cell nucleus. It has been proposed that coumarin derivatives enter the cell and alter the cell-division cycle [28, 29]. Antitumor properties may also be related to apoptotic inducing elements [28]. Paradoxically, some work suggests that coumarin metabolites may be toxic. Different species produce different coumarin metabolites resulting in variable levels of cytotoxicity. In humans, coumarins are often reduced to innocuous 7-hydroxycoumarin derivatives; alternatively, in rodents coumarins are metabolized via a C-3, C-4 epoxide intermediate (**15**) that is toxic [30, 31].

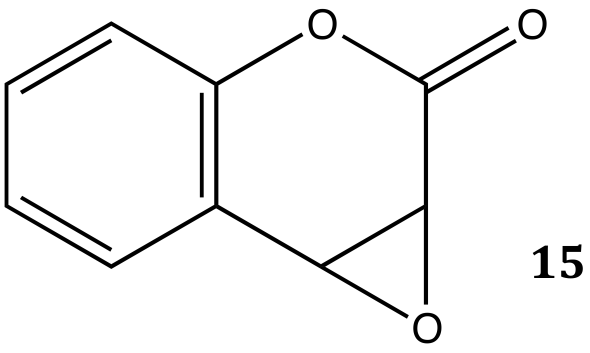

15

Figure 16. Coumarin 3,4-epoxide intermediate. A common, toxic coumarin metabolite in rodents [31].

Humans are regularly exposed to coumarins in beauty products and food, so some tolerable level of coumarin exposure does, indeed, exist [19].

In addition, previous work has suggested that a "set point" concentration of intracellular coumarin derivatives is necessary to reduce oxidative stress [19]. For

example, Novobicin, **9**, which has emerged as a promising anti-cancer agent, is a coumarin derivative that demonstrates anti-tumor properties. Its activity is attributed to the interaction between Novobicin and heat-shock protein 90 (Hsp90), a molecular chaperone protein that mediates the cellular response to stress. Molecular chaperones have emerged as critical regulatory molecules in the evolution of cancer. The relative concentrations of Hsp90 and Novobicin are thought to determine Novobicin's efficacy [19, 32]. Likewise, the relative concentrations of Vitamin K and Warfarin can influence the level of Warfarin's anticoagulant activity [33].

The current study investigates the influence of isoprenyl position and chain length on the cytotoxicity of isoprenyl coumarins against PANC-1 cells in nutrient-deprived conditions. Moreover, we propose to probe the underlying mechanisms of coumarin-derived bioactivity using fluorescence experiments. We are particularly interested in the structures that facilitate the selective bioactivity of coumarin derivatives in nutrient-deprived conditions. Our immediate goals are three-fold: 1) to synthesize two novel series of isoprenylated coumarins: a monoprenylated series substituted at the C-4 position (Figure 17) and a diprenylated series substituted at the C-4 and C-7 position (Figure 18), 2) to determine the bioactivity of these novel coumarins against healthy human fibroblast cells, and PANC-1 cells in nutrient-rich and nutrient-deprived conditions, and 3) to investigate the mechanism of coumarin cytotoxicity using fluorescence spectroscopy.

Most naturally occurring coumarins are substituted at the 6^{th}, 7^{th}, or 8^{th} carbons of the bicyclic structural backbone (Figure 8) and the primary coumarin metabolite in humans is 7-hydroxycoumarin [17, 33]. Additionally, recent work from our laboratory has demonstrated the promising cytotoxicity of coumarins substituted at the C-7 position [16]

against PANC-1 cells under nutrient deprived conditions. Consequently, prior research efforts have focused mostly on coumarins substituted at the 6th, 7th, and 8th positions, and strikingly little work has been done on the activities of C-3 and C-4 substituted coumarins. Thus, we selected to investigate the influence of isoprenyl positioning on anti-cancer activity by focusing on coumarins substituted at the C-4 position (Figure 17).

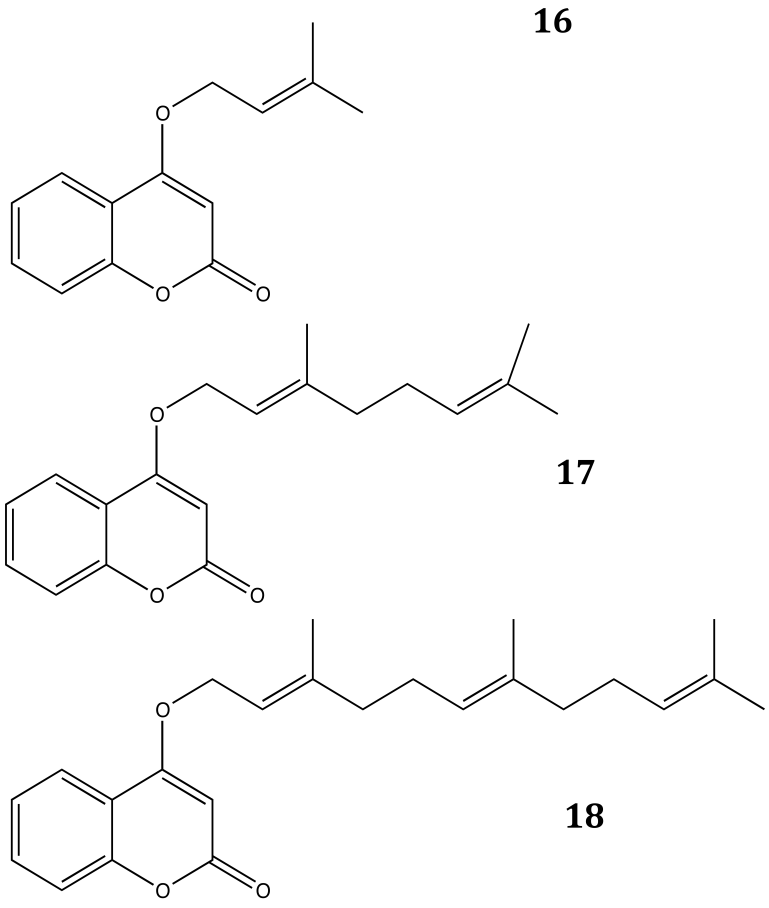

Figure 17. Proposed isoprenylated structures alkylated at the C-4 position (Series 1).

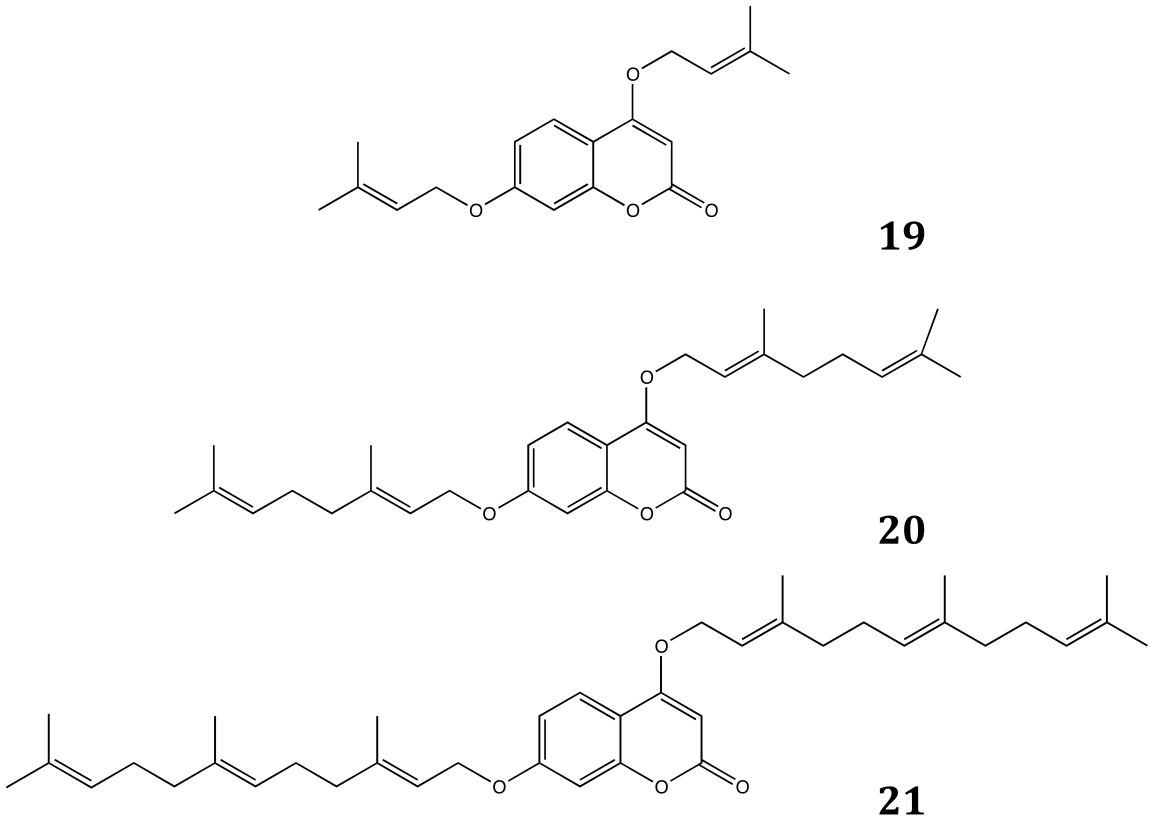

Figure 18. Proposed diprenylated structures alkylated at the C-4 and C-7 positions (Series 2).

In the present study, we will alkylate 4-hydroxycoumarin with isoprenyl moieties of varying length, using the Williamson Ether synthesis (Figure 19). The Williamson Ether synthesis employs commercially available halide starting materials and 4-hydroxycoumarin.

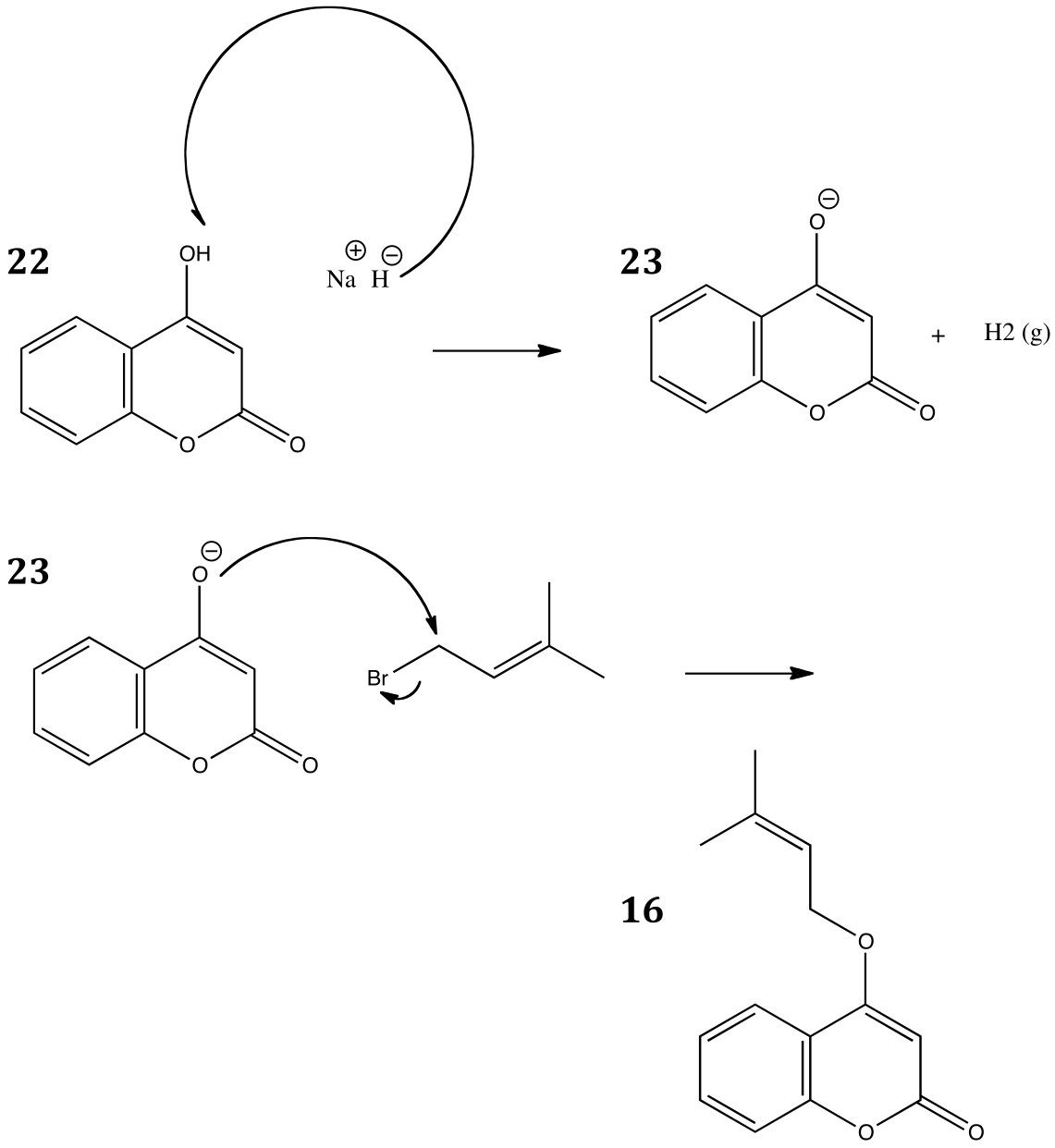

Figure 19. Schematic of Williamson ether synthesis. Starting materials consist of 4-hydroxycoumarin and a halogenated isoprenyl chain.

The mechanism proceeds as follows: first, sodium hydride is added to 4-hydroxycoumarin to depronate the hydroxy group; the alkyl halide is then added to the reaction mixture, allowing the deprotonated coumarin to displace the halide via an S_N2 reaction (Figure 19). The polar, aprotic solvent, DMF, allows the reaction to proceed in

good yield. The same mechanism was expected to proceed with a dihydroxy starting material.

In addition to evaluating the bioactivities of C-4 substituted coumarins, we will investigate the cytotoxicity of diprenylated coumarins, with substituents at the C-4 and C-7 positions and monosubstituted coumarins with saturated and partially saturated, chiral isoprenyl tails (Figures 19 and 20). These findings will inform our understanding of the effect of chirality, saturation and the introduction of an additional isoprenyl moiety on the underlying molecular mechanisms of activity. Each member of series 3 is substituted at the C-6 position by an isoprenyl chain made of 10 carbons. Compound **24** is fully saturated; whereas, **25** and **26** represent "R" and "S" enantiomers of the hydrocarbon chain (Figure 20). We propose to perform structure-activity relationship (SAR studies) on each of the newly synthesized coumarins, in nutrient rich and nutrient deprived conditions. Compounds will be tested against human pancreatic adenocarcinoma (PANC-1) cell lines, as well as healthy human fibroblasts to determine the specificity of cytotoxicity. Next, we will consider the intrinsic fluorescence of coumarin derivatives. If detectably fluorescent, we propose to localize our novel coumarin derivatives within PANC-1 cells, or at the external cellular membrane. Further, we will analyze the morphological changes that PANC-1 cells undergo following exposure to coumarin derivatives.

24

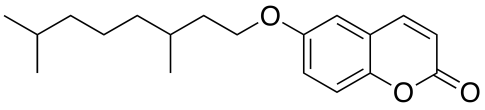

25

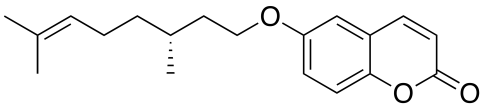

26

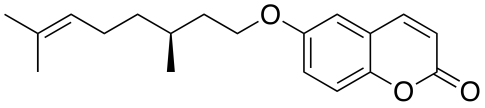

Figure 20. Structures of (Series 3) compounds that test the influence of chirality and saturation on bioactivity. **24** is a fully saturated coumarin derivative. **25,** the "R" enantiomer and **26**, the "S" enantiomer.

Results

Synthesis of isoprenylated coumarins via Williamson Ether synthesis

In order to evaluate the effect of isoprenyl positioning on coumarin-derived cytotoxicity against pancreatic adenocarcinoma (PANC-1) cell lines, we attempted to synthesize two novel series of isoprenylated coumarins from the starting materials 4-hydroxycoumarin (**22**) and 4,7-dihydroxycoumarin (**27**).

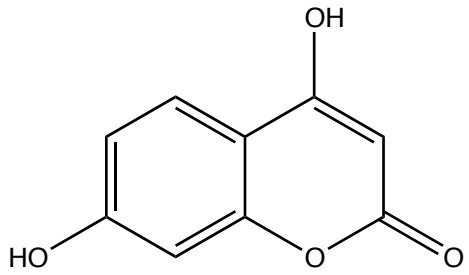

27

Figure 21. Chemical structure of the starting material, 4,7-dihydroxycoumarin.

Previously, the Williamson Ether synthesis (Figure 19) was employed to synthesize similarly substituted coumarins from hydroxycoumarin starting materials in good yield [16]. So, we selected to use the same reaction procedure to alkylate 4-hydroxycoumarin (**22**) and 4,7-dihydroxycoumain (**27**). Given the structural similarities between the hydroxycoumarins and halogenated isoprenyl substrates, the same reaction procedure, with slight modifications, was used to synthesize all targets.

Synthesis of Series 1: C-4 monoprenylated coumarins

The first attempt to alkylate 4-hydroxycoumarin (**22**) with 3,3-dimethylallylbromide was unsuccessful (the reaction mechanism is depicted in Figure 19). The reaction was set up using a previously described procedure and allowed to run overnight [16]. Reaction progress was monitored by thin layer chromatography. After 24 hours, the formation of three new spots suggested that the reaction had been successful and the reaction was stopped. When the crude mixture was developed in a 7:3; Hexanes: Ethyl (H:E) acetate solvent system, the newly formed spots exhibited rf values of 0.32, 0.56 and 0.79, respectively. The second spot (rf = 0.56) was suspected to be the desired product; though its rf value was higher than the expected value (0.41). To purify the suspected product band, the crude reaction material was loaded onto a preparative thin layer chromatography plate and developed in a 7:3; H:E solvent system. When the separated bands were visualized using ultraviolet light, no distinct bands were visible. Rather, there was one smeared band that spanned from the loading position to the solvent front. This smear was later attributed to excess N,N-dimethylformamide (DMF), the reaction solvent. Consequently, all organic material was retrieved from the plate and further concentrated *in vacuo*. To confirm the viability of the retrieved material, the mixture was separated on a TLC plate. However, this separation produced six new spots, indicating that the products had decomposed prior to separation. To minimize excess solvent without significantly increasing the work-up time, half of the initial volume of DMF was used in later iterations of this reaction.

The second attempt to alkylate **22** with 3,3-dimethylallylbromide produced three new spots on the reaction TLC. The crude mixture was again separated by preparative

TLC and the resultant bands exhibited rf values of 0.63, 0.43 and 0.15. The suspected product band (rf = 0.43) was recovered from the plate and identified as the desired product via ^{1}H-NMR analysis (Appendix I). The purity and identity of this compound was later confirmed by ^{13}C-NMR and high-resolution mass spectroscopy (HRMS) (Appendices II, IX, X).

Upon successful completion of the first alkylation reaction, the same procedure was used to produce two similar coumarin derivates (**17** and **18**). Notably, geranyl bromide and farnesyl bromide, the halogenated electrophiles, are light sensitive. As such, reactions were run with minimal exposure to light. The first attempt to alkyate 4-hydroxycoumarin with geranyl bromide was successful, and produced one new product spot with an expected rf value of 0.51 by TLC analysis. However, the crude mixture was mistakenly loaded onto a non-fluorescent preparative TLC plate and decomposed before it could be purified. The second attempt to synthesize **17** was successful. But, again, the isolation of the desired product failed. During the purification of the desired product via preparative TLC, the product band migrated with that of the decomposed bromide due to a wide loading band (Figure 22**).** Both bands were recovered and again separated using preparative TLC; though, the product decomposed before it was separated from the bromide band in a 10:1 Hexanes:Ethyl Acetate solvent system. Later preparative TLCs were loaded with thinner bands and exposed to heat prior to development to improve resolution quality.

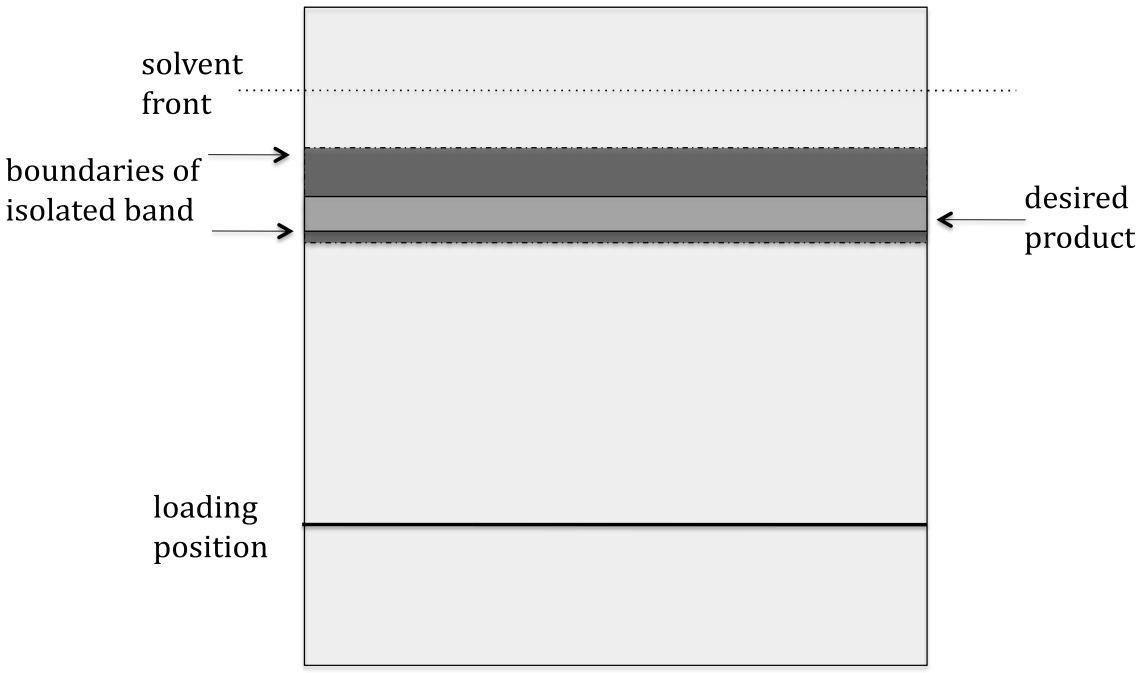

Figure 22. Schematic diagram depicting desired product (indicated by dark gray) obscured by a wide band (indicated by light gray).

The third attempt to synthesize and purify **17** was successful and its identity was confirmed by ^{1}H-NMR analysis, ^{13}C-NMR analysis and HRMS (Appendices III, IV, XI, XII). The same reaction procedure was used to synthesize **18**, which was purified by preparative TLC and characterized by ^{1}H-NMR analysis, ^{13}C-NMR analysis and HRMS (Appendices V, VI, XIII, XIV). Characteristic peaks produced by the methylene (indicated in pink) and allylic (indicated by green and blue) protons of the isoprenoid moiety were used to identify the desired products (Figure 23).[a]

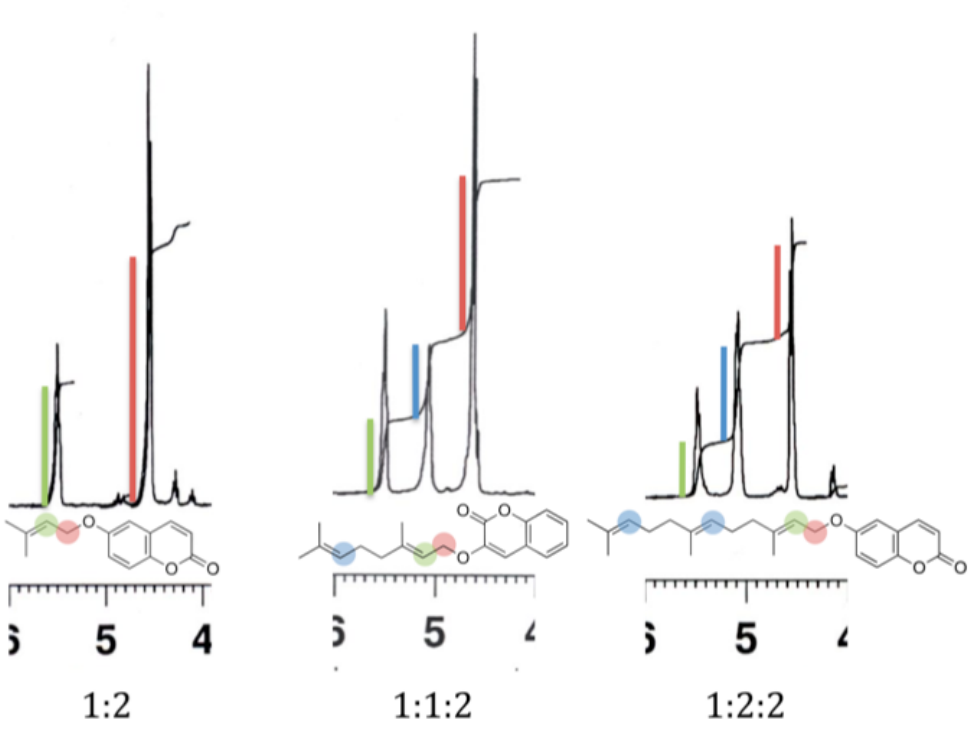

Figure 23.[a] Representative depiction of signature H-NMR peaks from previously characterized compounds. Blue color-coded protons represent distal allylic hydrogens, while green color-coded protons correspond to the allylic proton most proximal to the coumarin ring. The red color indicates methylene protons. The integration values are shown underneath each signal. [a]This figure was created by Maria Jun '16 and Alyssa Bacay '16.

Synthesis of C-4,7 diprenylated coumarins

Synthesis of the diprenylated coumarins was attempted using the same Williamson ether synthesis as the monoprenylated series, with double the molar quantities of sodium hydroxide and isoprenyl halide (Figure 19). Reaction progress of the first diprenylation reaction, where two equivalents of 3,3-dimethylbromide were reacted with 4,7-dihydroxycoumarin, was, monitored via TLC. The formation of two new product spots (rf = 0.63 and 0.81) suggested that the reaction was successful, and the remaining two diprenylation reactions were set up in tandem. The C10 diprenylation reaction mixture produced three product spots (rf = 0.46, 0.56 and 0.77), suggesting that the reaction may have been successful. The rf value of the C5 diprenylation product, **19,** was expected to be higher than the rf value of the monoprenylated C5 product (**16**), 0.41, so the third band (rf=0.81) was further characterized by H-NMR. Band 3 produced H-NMR peaks that corresponded to each of the aromatic protons and had a peak at 4.8 ppm with an integration of 2, rather than the 4 anticipated methylene protons (Appendix VIII). In addition, the possible allylic peak appeared further upfield than expected (4.9 instead of 5.5 ppm)(Appendix VII). The product corresponding to band 2 was then characterized by H-NMR. Oddly, band 3 produced NMR peaks at the correct chemical shift (4.8 ppm), with the correct integration for the methylene protons, but no peak appeared around 5.5 ppm, the chemical shift of the most up-field aromatic proton (Appendix VIII). Because the C5 diprenylation product could not be identified, the remaining diprenylation products were not further characterized or used in biological testing. Reaction TLC of the C-15 diprenylation product was prevented by the thickness of the reaction mixture, so it

is unclear how many products were formed. In contrast to previous reaction mixtures, the C-15 diprenylation product appeared as a thick, oily mass; whereas, previous reaction mixtures were colored liquids. This change in reaction mixture consistency may be explained by the significant hydrophobicity of **24** compared to other structures.

To improve our understanding of the molecular mechanisms underlying coumarin-derived cytotoxicity, we also investigated the bioactivities of three compounds that were previously synthesized by another member of the Carrico-Moniz lab, Christine Chun '15 (**24, 25, 26**). This third series of compounds was engineered to test the influence of chirality and saturation on cytotoxicity against PANC-1 cells. All series 3 compounds were characterized by H-NMR, C-NMR and HRMS (Appendices 15-26).

Biological Results

The bioactivities of each of the fully characterized coumarins were tested using a previously described colorimetric viability assay [16]. Mechanistically, the assay makes use of an endogenous dehydrodrogenase that reduces a yellow WST-8 salt, causing the dye to change color (orange) and absorb light at 450 nm. The enzyme is only present in viable cells, so WST-8 is not reduced in compromised cells. Absorbance at 450 nm, attributed to the reduced WST-8 dye, is directly proportional to the number of viable cells remaining in each well (Figure 24).

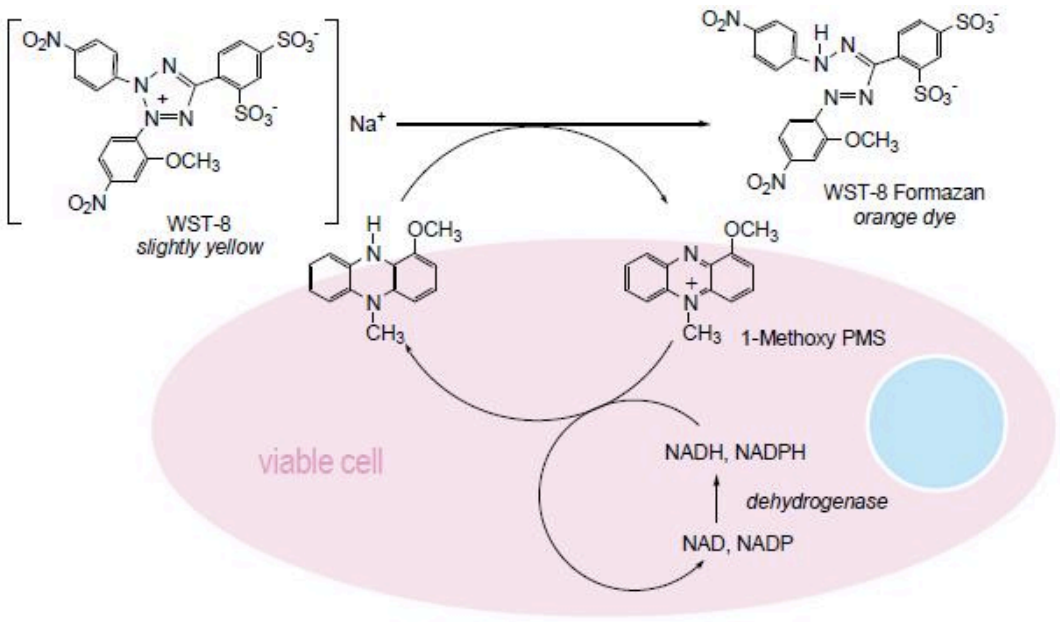

Figure 24. Schematic representing the mechanism underlying the colorimetric assay, reprinted from Dojindo©.

In the first cell viability assay, **16** and **17**, were tested against PANC-1 cells in nutrient deprived (NDM) and nutrient rich (NRM) conditions. The results from the first viability assay were largely inconclusive, though they suggest pronounced cytotoxicity for compound **17** (Figure 25). To facilitate the analysis of cytotoxicity as a function of isoprenyl chain length, compounds are henceforth referred to, interchangeably, by the number of carbons in their isoprenyl tails (for instance, **16** has 5 carbons in its substituent and is thus referred to as C5).

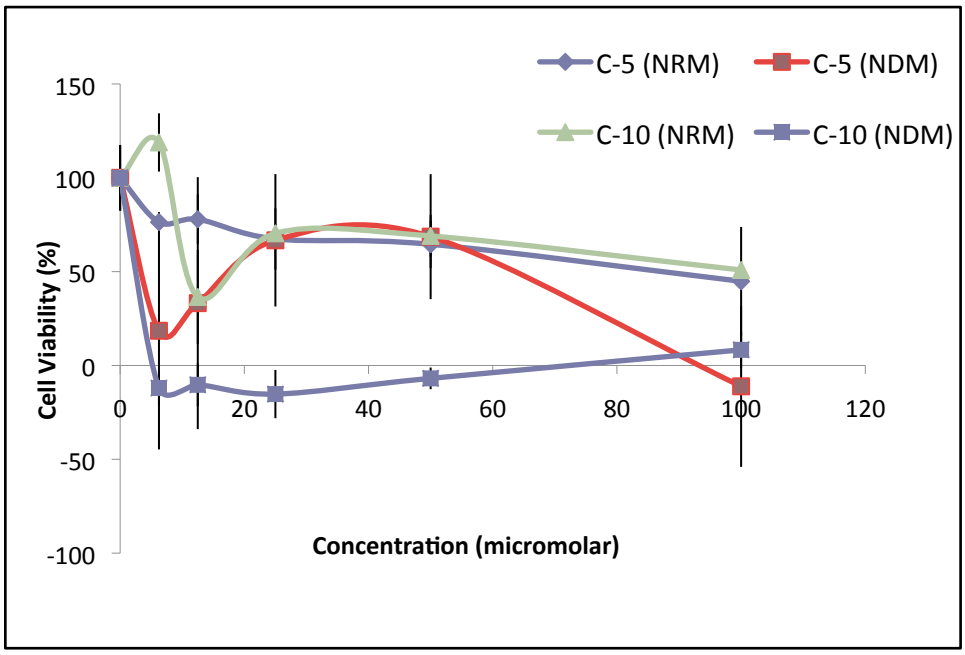

Figure 25. PANC-1 cell viability in nutrient-deprived and nutrient-rich conditions following 24-hour incubation with coumarin derivatives, **16** and **17**. Error bars indicate standard error of the mean (SEM). C5 refers to **16**. C10 refers to **17**. NDM indicates nutrient-deprived media and NRM indicates nutrient-rich media.

As anticipated, **16** had little effect on the viability of PANC-1 cells in NRM conditions (Figure 25). Surprisingly, though, at 100 μM both **16** and **17** were found to reduce cell viability to approximately 0%. Indeed, **17**, exhibited potent cytotoxicity against PANC-1 cells in NDM at all concentrations, with an LC_{50} value of approximately 3.5 μM. Significant variability within the readings suggests that there may have been issues with compound solubility. To resolve outstanding questions regarding the effect of **17** and **18** on cell viability, the assay was repeated (Figure 26).

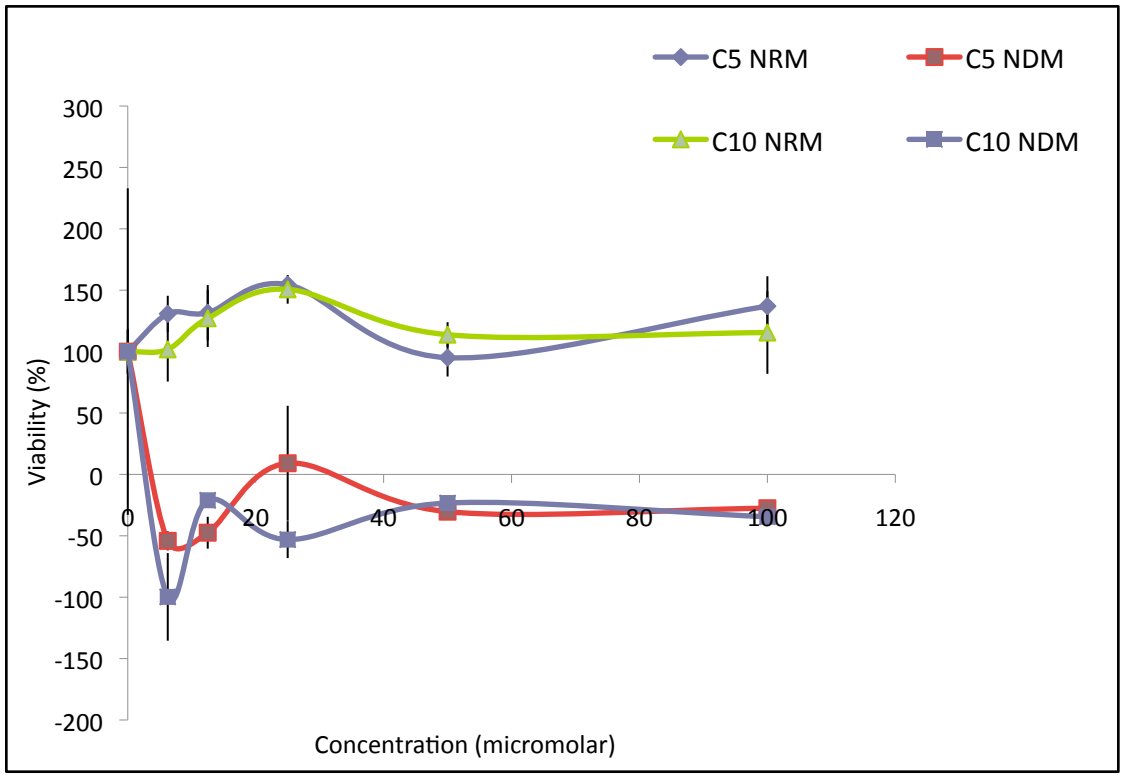

Figure 26. PANC-1 cell viability in nutrient-deprived and nutrient-rich conditions following 24-hour incubation with coumarin derivatives, **16** and **17**. Error bars indicate standard error of the mean (SEM). C5 refers to **16**. C10 refers to **17**. NDM indicates nutrient-deprived media and NRM indicates nutrient-rich media.

To our satisfaction, the variability in each of the conditions diminished in the repeated assay, suggesting that we were able to resolve solubility issues from the previous assay. These data suggest a clear trend towards specific and pronounced cytotoxicity in nutrient-deprived conditions, but not nutrient-rich conditions, for both **16** and **17**. Compounds **16** and **17** exhibited an LC_{50} value of 3.5 μM, corroborating the results of the first assay regarding **17** (Figure 25). No consistent pattern was observed for the bioactivity of **16**. This inconsistency underscored the need for yet an additional assay, the results of which are shown here (Figures 27-28). At present, we report only the results for the third C10 assay.

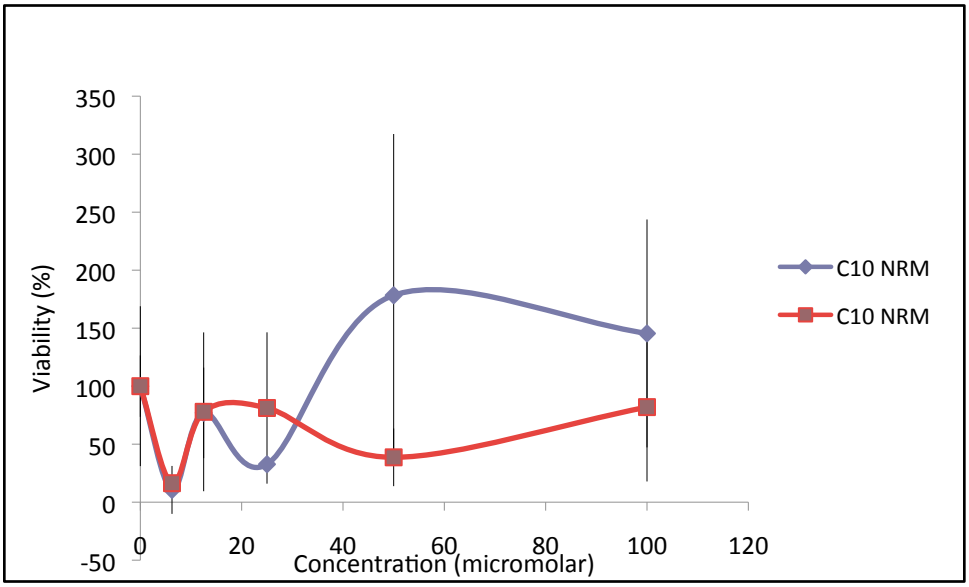

Figure 27. PANC-1 cell viability in nutrient-rich media conditions following a 24-hour incubation period with **17**. Error bars indicate standard error of the mean (SEM). C10 refers to **17**. NRM indicates nutrient-rich media.

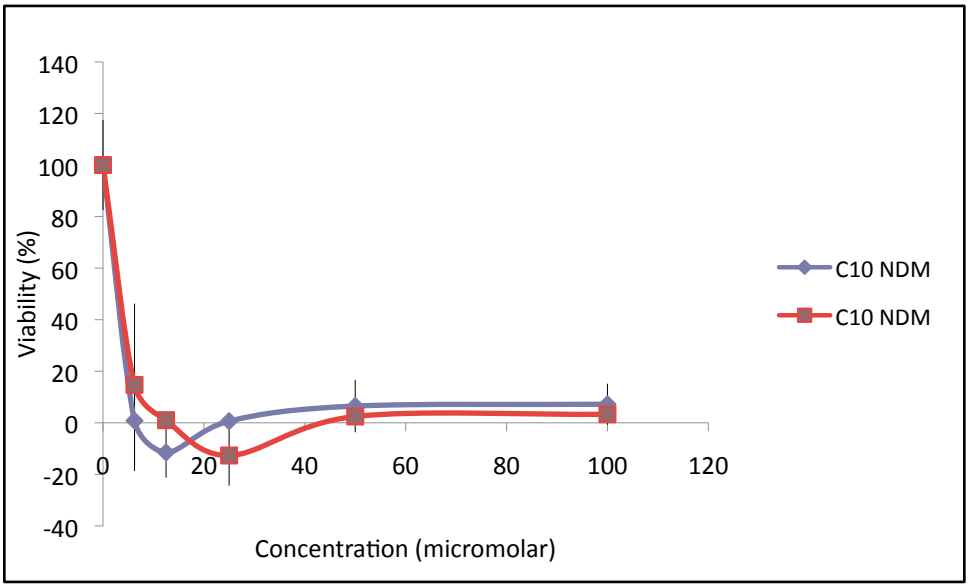

Figure 28. PANC-1 cell viability in nutrient-poor media conditions following a 24-hour incubation period with **17**. Error bars indicate standard error of the mean (SEM). C10 refers to **17**. NDM indicates nutrient-deprived media.

These data suggest that the activity of **17** varies between nutrient-rich and nutrient poor conditions and confirm its LC_{50} value (Figures 25 and 26). Interestingly, experimental variability, as measured by the standard error of the mean, also seems to vary between the two media conditions. This may suggest that compound **17** is more soluble in nutrient-deprived conditions than in nutrient-rich conditions. Alternatively, these findings may demonstrate that **17** has variable bioactivity in PANC-1 cells in nutrient-rich media conditions. Compound **18** exhibited an LC_{50} value of 6 μM against PANC-1 cells in nutrient-deprived, but not nutrient-rich conditions (Figure 29).

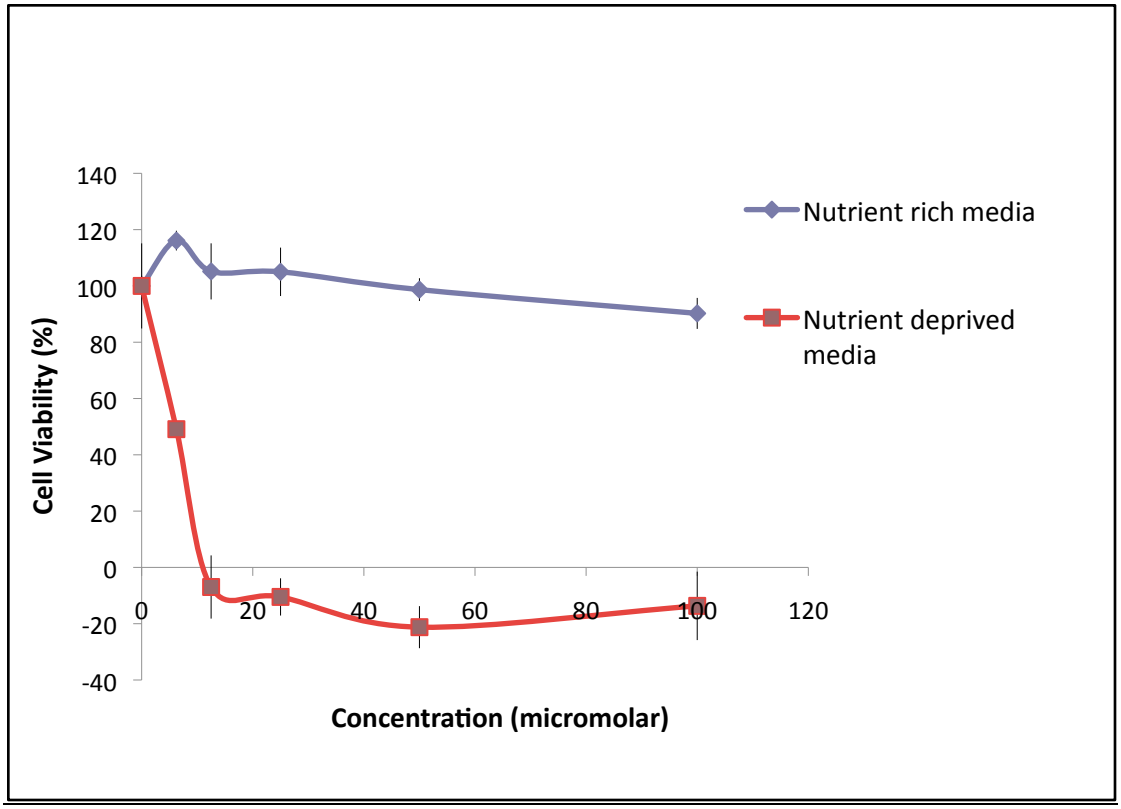

Figure 29. PANC-1 cell viability in nutrient-deprived and nutrient-rich conditions following 24-hour incubation with coumarin derivative, **18**. Error bars indicate standard error of the mean (SEM). C15 refers to compound **18**.

These results were replicated and produced the same LC_{50} value of 6 μM (Figure 30).

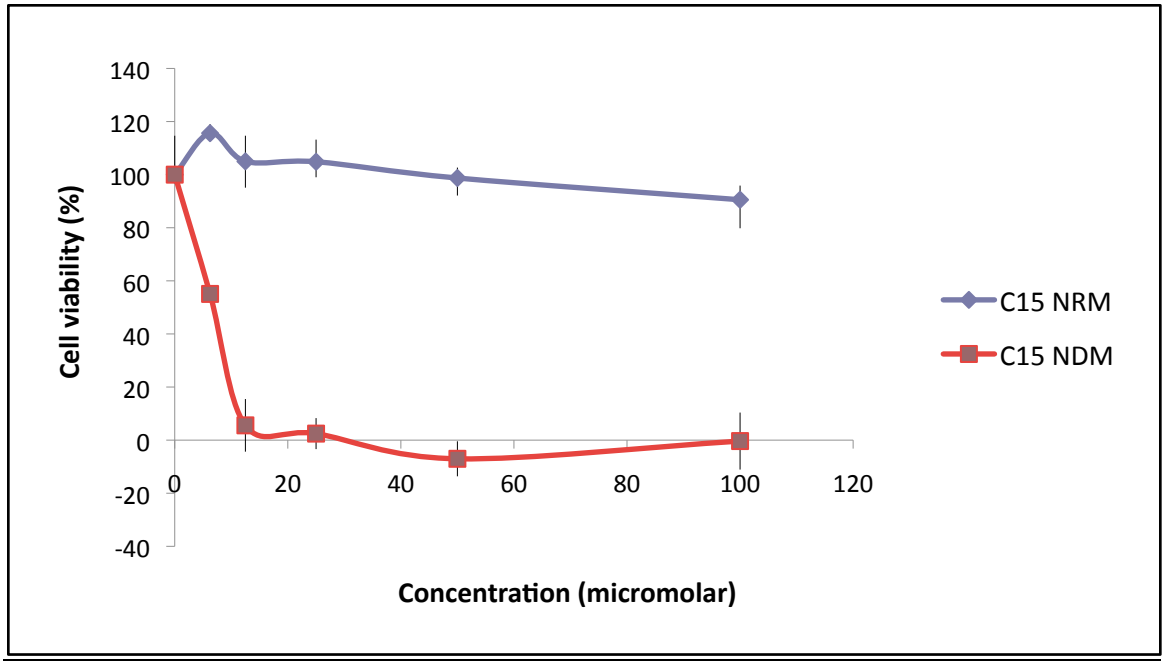

Figure 30. PANC-1 cell viability in nutrient-deprived and nutrient-rich conditions following 24-hour incubation with coumarin derivative, **18**. Error bars indicate standard error of the mean (SEM). C15 refers to compound **18**. NDM indicates nutrient-deprived media and NRM indicates nutrient-rich media.

It is interesting to note that variability was high in the C5 and C10 assays, but minimal in the C15 assays. This trend, in which longer isoprenyl tails lead to less variability, may suggest that the variability was not due to solubility alone.

The fully saturated coumarin derivative, **24**, produced inconsistent results that were not concentration-dependent (Figure 31).

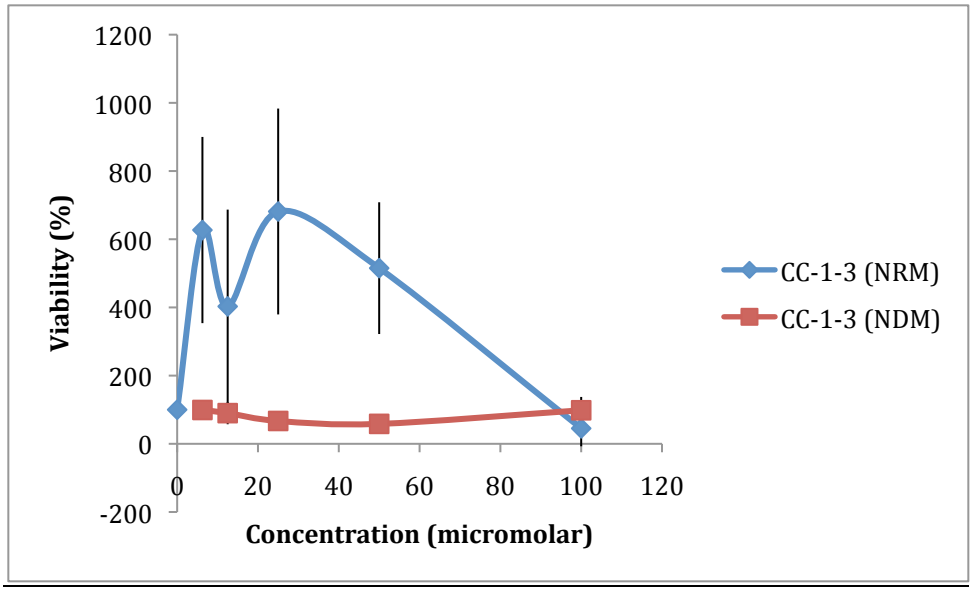

Figure 31. PANC-1 cell viability in nutrient-deprived and nutrient-rich conditions following 24-hour incubation with coumarin derivative, **24** (CC-1-3). Error bars indicate standard error of the mean (SEM). NDM indicates nutrient-deprived media and NRM indicates nutrient-rich media.

Unfortunately, the variation in these data make it difficult to draw conclusive results. Nevertheless, even high concentrations of the compound did not significantly reduce cell viability by more than 50%, suggesting that complete saturation reduces cytotoxicity of coumarin derivatives (Figure 31).

The "R" enantiomer, **25**, also did not exhibit a concentration-dependent effect on PANC-1 viability. In fact, the cytotoxicity trend is the opposite of what was expected—cytotoxicity decreased with increasing concentration (Figure 32). Again, variability in the data acquired was high.

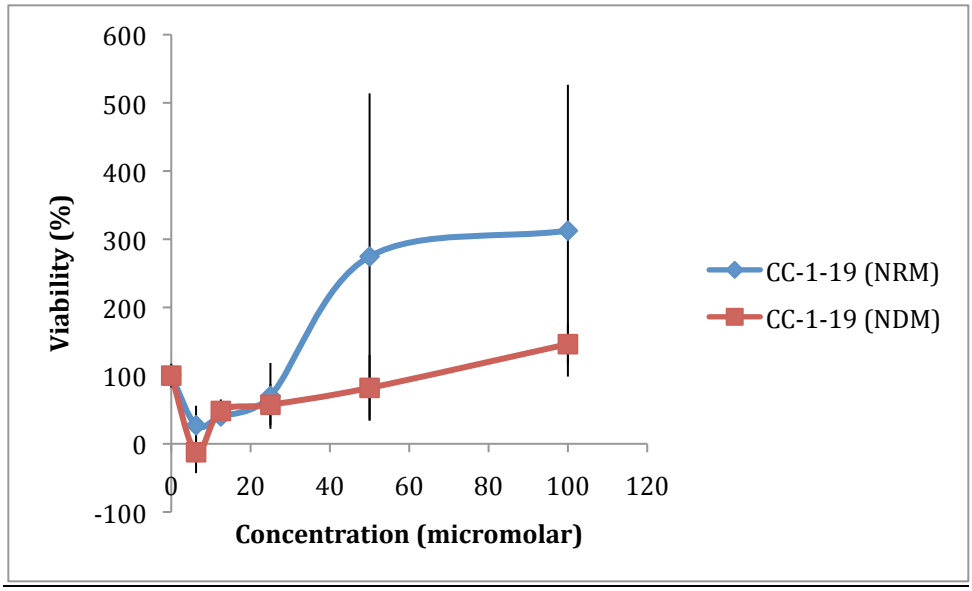

Figure 32. PANC-1 cell viability in nutrient-deprived and nutrient-rich conditions following 24-hour incubation with coumarin derivative, **25** (CC-1-19). Error bars indicate standard error of the mean (SEM). NDM indicates nutrient-deprived media and NRM indicates nutrient-rich media.

Alternatively, the "S" enantiomer appeared completely innocuous in both nutrient-deprived and nutrient-rich conditions (Figure 33). In both media conditions, cell viability fluctuated about 100% viability indicating that **26** was not toxic to PANC-1 cells (Figure 33).

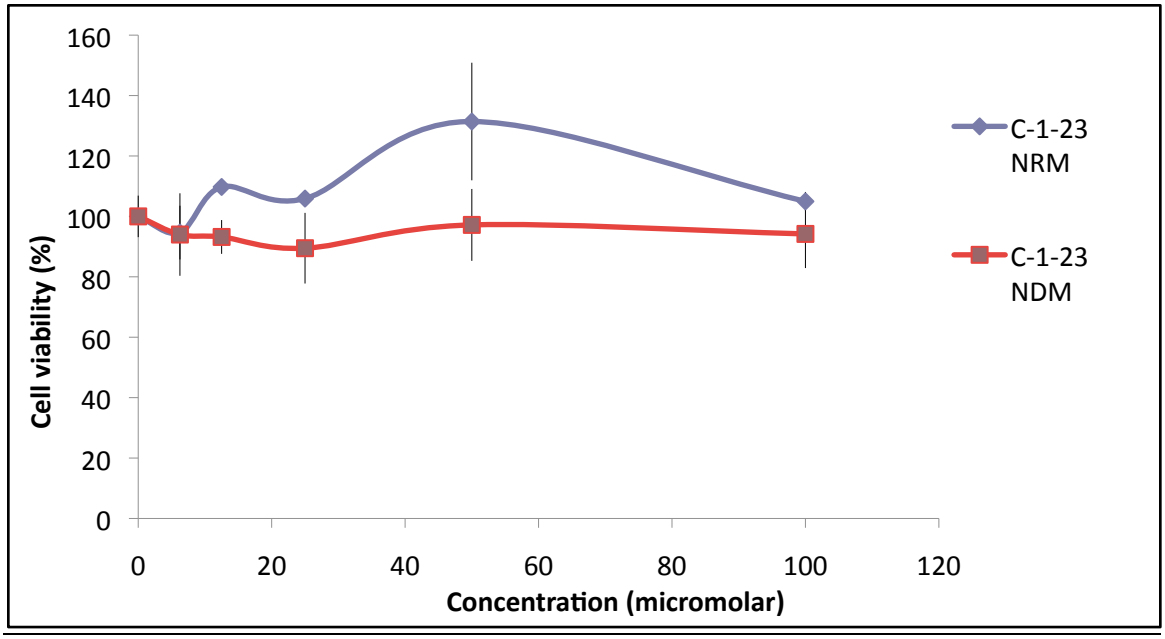

Figure 33. PANC-1 cell viability in nutrient-deprived and nutrient-rich conditions following 24-hour incubation with coumarin derivative, **26** (CC-1-23). Error bars indicate standard error of the mean (SEM). NDM indicates nutrient-deprived media and NRM indicates nutrient-rich media.

In sum, the C10 monoprenylated compound exhibited the lowest LC_{50} value (3.5 μM) of all the compounds tested against PANC-1 cells in nutrient-deprived media. The second most toxic compound was the C15 monoprenylated product with an LC_{50} value of 6 μM. No definitive trend was identified for the C5 monoprenylated product. Our preliminary work suggests that none of the series 3 compounds demonstrated concentration-dependent cytotoxicity against the PANC-1 cells.

Discussion

The present study sought to describe the influence of substitution position, substituent chain length (Series 1) and diprenylation (Series 2) on the cytotoxicity of simple coumarin-derivatives against PANC-1 cells in nutrient-deprived and nutrient-rich media conditions. To this end, we synthesized a novel series of coumarin derivatives substituted with isoprenyl moieties of varying length at the C-4 position. Moreover, we attempted to synthesize a series of diprenylated coumarins, substituted with varying isoprenyl moieties at the C-4 and C-7 positions. The bioactivity of previously characterized compounds (Series 3) was also considered as a proxy for the influence of chirality and saturation on cytotoxicity. The underlying cause for pancreatic cancers' resistance to nutrient deprivation remains unknown. However, this austerity in nutrient-poor environments creates a novel biochemical target in the treatment of pancreatic cancer. Structure-activity relationship studies, like this one, pose another way of understanding this resistance to nutrient-deprivation and thus using it to develop novel therapies.

Herein, we report the synthesis and characterization of a novel series of monoprenylated coumarins substituted at the C4 position with 5, 10 and 15 carbon isoprenylated chains. Each of these compounds was fully characterized by ^{1}H-NMR, ^{13}C-NMR and HRMS prior to biological testing. The bioactivities of each of these compounds was assayed against PANC-1 cells in nutrient-rich and nutrient-deprived conditions and each of these assays was replicated at least twice. We attempted to synthesize an analogous series of diprenylated coumarins; however, the Williamson ether synthesis underwent an unexpected side reaction and the formation of the desired product

was inconclusive. The monoprenylated series (Series 1), in addition to three previously synthesized compounds, were tested in our viability assay to determine the influence of isoprenyl chain positioning, saturation and chirality on cytotoxicity.

Of the compounds tested, coumarin derivatives substituted at the C-4 position, with substituents of 10 or 15 carbons in length proved most cytotoxic. Compounds **17** and **18** exhibited LC_{50} values of 3.5 and 5 μM, respectively. This finding is surprising given our previous work that has directly correlated chain length with cytotoxicity [16]. Nevertheless, multiple repetitions of the relevant assays have confirmed our initial finding that the C10 compound is more cytotoxic than the C15 derivative (Figures 25, 26, 28-30). This discrepancy may be explained by the fact that substitution position does, indeed, influence bioactivity and potentially the underlying mechanism of action. Previous work has suggested that derivatives with short isoprenyl substituents (of 5 carbons, specifically) are generally nontoxic to PANC-1 cells in nutrient-deprived media [16]. Our preliminary findings, while variable, suggest that the C5 derivative has some cytotoxicity against PANC-1 cells in NDM. The results of the first assay were inconclusive, though the C5 compound was toxic to cells at 100 μM (Figure 25). Surprisingly, the second assay indicated an LC_{50} value of approximately 3.5 μM (Figure 26). Future work will replicate biological assays with the C5 compound to confirm its bioactivity against PANC-1 cells during nutrient deprivation.

Upcoming studies will propose novel synthetic schemes for the diprenylation reaction (Series 2). Further characterization of our previously formed side products will inform these variations. The successful synthesis of a series of diprenylated products will contribute to our understanding of what structural components underlie coumarin-derived

cytotoxicity, by further probing the influence of size, hydrophobicity and substitution position on bioactivity. Preliminary biological results from probing the activity of series 3 compounds suggest that chirality and saturation may not be critical structural elements for cytotoxicity. Both enantiomers of the C10 coumarin, substituted at the C-6 position, compounds **25** and **26**, and its fully saturated analogue, compound **24**, reduced cell viability by no more than 50%, even at concentrations of 100 μM (Figures 31-33). These findings were not duplicated and are therefore not yet conclusive. Future assays are therefore necessary to confirm these initial results.

While the development of coumarin derivatives as anti-pancreatic cancer agents is still in its infancy, this study provides valuable information about the structural elements that are necessary for coumarin-derived bioactivity. Our findings confirm that simple coumarin-derivatives can exhibit robust cytotoxicity against PANC-1 cells nutrient deprived conditions at low micromolar concentrations. We posit that increasing substituent length, and thereby hydophobicity, may not be the sole factor in increasing cytotoxicity. Indeed, **17**, a coumarin with an isoprenoid group of 10 carbons in length was more toxic than derivatives with longer isoprenyl groups at the C-4 or C-7 position (Figure 28, [16]). As such, the observed increase in cytotoxicity appears to result from a delicate balance of substituent length/hydophobicity, saturation and proper positioning on the coumarin scaffold. In this study, structural analogs with isoprenyl substituents of the same length as **17** (compounds 24, 25 and 26, which were fully saturated or partially saturated and chiral) reduced cell viability by only 50%.

The physiological target of these coumarin derivatives remains unclear. Of the compounds analyzed in this study, the C15 derivative, compound **18**, was selected for

future fluorescence studies due to its robust intrinsic UV-fluorescence (data not shown). Future work will make use of this intrinsic fluorescence to localize coumarins within the cell or at the membrane surface. The first step towards identifying the physiological target of our compounds will be to determine the peak excitation and emission wavelengths for one of our synthesized coumarins (likely the C15 monoprenylated derivative). Once we are able to selectively excite and detect our compound, we can monitor compound fluorescence while quenching fluorescence outside the cell using dye. If the compound remains detectable after the fluorescence quench, it suggests that the coumarin derivatives do, indeed, cross the cell membrane and enter the cell.

In the evolution of coumarin-derived therapies in the treatment of pancreatic cancer, a number of outstanding control experiments remain:

To confirm compound solubility over time and verify our biological data, we propose measuring compound concentration in the media/DMSO solution, using Beer's Law. Verifying compound solubility could also support or refute the suggestion that variable compound solubility is producing variable biological results (as in the case of the C5 monoprenylated product).

Future work will also confirm the specificity of coumarin-derived cytotoxicity against pancreatic cancer cells by testing these compounds against non-cancerous cells, specifically healthy human fibroblasts (WI-38, ATCC). We also propose to assay our compounds against other lines of pancreatic cancer cells to confirm that this cytotoxicity is not the result of something unique to PANC-1 cells.

To improve the accuracy of our biological assay and produce results that are more physiologically relevant, we propose excluding data that does not meet specific

constraints. For instance, it is expected that the 0 μM control (which contains cells, media and kit) should absorb more energy at 450 nm than the blank control (which contains only media and kit) due to the presence of cells. However, some of our data violates this assumption, leading to impractically high cell viabilities (300%+) and negative viabilities (Figures 31 and 32). Whatever the reason for these discrepancies, they suggest that the colorimetric assay is not working as expected. The WST-8 colorimetric assay depends on the activity of a dehydrogenase associated with the cellular energy production. This pathway may be compromised in nutrient-deprived conditions, skewing the results of our biological assays. It is critical to confirm that dehydrogenase activity is not altered in nutrient deprived conditions, independent of coumarin bioactivity, altering our results. To circumvent these problems, we suggest measuring cell viability using other methods. Moreover, we are interested in whether or not cells shocked into nutrient deprivation (as is currently the case in our biological assay) respond to coumarin derivatives in same way as those that are accustomed to nutrient deprivation. To better simulate the tumor microenvironment, we suggest co-culturing cancerous and healthy cells together, and inducing the growth of tumor cells into spheroids (or 3D balls of cells). The use of co-cultured spheroids would allow us to model coumarin diffusion into the tumor core, while exploring compound interactions with the two cell types. The completion of the aforementioned controls will provide robust evidence for the specific bioactivity of coumarin derivatives against pancreatic cancer cells in nutrient-poor conditions. This specific cytotoxicity can then be harnessed as a novel biochemical treatment for pancreatic cancer tumors.

Conclusion

Herein, we report the synthesis of a novel series of monoprenylated coumarins, substituted at the C-4 position of the coumarin scaffold with 5, 10 and 15 carbon tails. The cytotoxicity of these coumarin derivatives was tested against pancreatic adenocarcinoma (PANC-1) cell lines, in nutrient-rich and nutrient-poor conditions. These derivatives proved toxic in nutrient-deprived conditions and innocuous in nutrient-rich conditions. Coumarins with isoprenyl tails of 10 and 15 carbons in length exhibited LC_{50} values of 3.5 and 6 μM, respectively, in nutrient-deprived conditions. We attempted to synthesize a second series of diprenylated coumarins with substituents at the C-4 and C-7 positions; however, our initial syntheses were unsuccessful. We also tested the bioactivity of a third series of coumarins substituted at the C-6 position with fully saturated and partially saturated, chiral tails. Series 3 compounds did not reduce cell viability by more than 50%, even at concentrations of 100 μM.

Previously, our lab has shown that isoprenyl chain length is directly correlated with cytotoxicity in coumarins substituted at the C-7 position [16]. Nevertheless, the results of the present study suggest that the influence of chain length on cytotoxicity is qualified by substituent position. Indeed, coumarins substituted at the C-4 position with a 10 carbon tail proved more toxic than derivatives substituted at the C4 and C7 positions with 15 and 20 carbon tails, respectively [16]. Moreover, these results suggest that chirality and saturation are inessential structural elements for coumarin-derived cytotoxicity.

Experimental section

General Protocols

^{1}H and ^{13}C NMR spectra were recorded on a
Bruker 300 Fourier transform instrument as dilute solutions in acetone-d_6 at 300 MHz (^{1}H NMR) or 75 MHz (^{13}C NMR). Chemical shifts were reported in δ (ppm) relative to tetramethylsilane. Reactants, reagents, and solvents were obtained from Sigma-Aldrich and were used as received. Synthesized final compounds were checked for purity by TLC analysis, ^{1}H NMR and ^{13}C NMR. High-resolution mass spectra (HRMS) and low-resolution mass spectra (LRMS) were performed on a 70-VSE or QTof Ultima mass spectrometer at the University of Illinois at Urbana-Champaign. Silica gel 60, F254, pre-coated glass TLC plates purchased from EMD were used for all (non-preparative) thin layer chromatography. Preparative thin layer chromatography was performed using pre-coated plates with 1000 microns thick silica gel coating purchased from Sigma Aldrich. Nutrient-rich and nutrient-deprived media were made from scratch based off of a previously published study[8]. The ingredients may be found in Appendix XXVII. In all cases, media pH was maintained at 7.4.

Cell culture protocol

All cell lines (PANC-1 and WI-38) were obtained from the ATCC and cultured in a 5% humidified CO_2 incubator at 37°C in complete DMEM (Sigma, Appendix XXVII). Cells were grown until a single layer of confluent cells had adhered to the flask and then were passaged into a new flask. The passaging procedure is as follows: First, old media is discarded via vacuum suction. Confluent cells are washed with room-temperature PBS, which is then discarded. Subsequently, 2-5 mL of thawed trysin-EDTA solution is filtered and added to the flask, prior to incubation at 37°C for 2-3 minutes. Once the majority of the cells are detached from the flask, the solution is transferred to a centrifuge tube and spun at 1000 rpm for 3 minutes. The resultant supernatant is discarded and the cell pellet is thoroughly resuspended in 2-4 mL of complete DMEM (Sigma). Cell suspension is transferred to a sterile flask and complete DMEM is added, as appropriate, prior to overnight incubation. The following day, cells are checked for attachment to the flask and allowed to grow for 3-4 days.

Experimental

Synthesis of 4-((3-methylbut-2-en-1-yl)oxy)-2H-chromen-2-one **(16)**

An oven-dried 50mL round bottom flask was prepared with a magnetic stirring bar, a rubber septum cover, and a nitrogen inlet. 4-hydroxycoumarin (**24**) (168 mg, 1.03 mmol) and 4 mL of anhydrous N,N-dimethylformamide (DMF) were added to the round bottom flask, which was again evacuated and purged with nitrogen. The solution was stirred and cooled to 0ºC in a salt-ice bath. Sodium hydride (48 mg of 60% mineral oil suspension, 2 mmol) was added to the flask, at which point H_2 gas began to form. The solution was then stirred at 0ºC for 30 minutes, under nitrogen gas. 3,3-dimethyl bromide (250 µL, 1.29 g/mL, 2.1 mmol) in 1 mL of anhydrous DMF was cooled to 0ºC and added drop-wise to the flask through the rubber septum using a syringe. The reaction mixture was left to stir under nitrogen and warm back to room temperature overnight. The desired product was obtained by preparative thin layer chromatography using a solvent system of 70% hexanes and 30% ethyl acetate (rf = 0.43). The purified product was verified by NMR spectroscopy (^{1}H-NMR, ^{13}C-NMR) and high-resolution mass spectrometry (HRMS). ^{1}H-NMR (300 MHz, $(CD_3)_2CO$): ∂ 1.81-2.06 (10H), 4.81-4.84 (s, 2H), 5.61 (m, 1H), 5.78 (s, 1H), 7.29 – 7.35 (m, 2H), 7.60 – 7.66 (m, 1H), 7.81-7.84 (m, 1H)**;** ^{13}C-NMR (75 MHz, $(CD_3)_2CO$): ∂ 18.14, 18.31, 25.85, 26.66, 67.19, 91.47, 116.73, 117.03, 117.27, 118.81, 123.15, 123.88, 124.52, 125.70, 132.21, 133.27, 140.63, 154.34, 162.30, 165.87. HRMS (ESI) Calcd. for $C_{14}H_{15}O_3$: 231.1021; found: 231.1022.

Synthesis of (E)-4-((3,7-dimethylocta-2,6-dien-1-yl)oxy)-2H-chromen-2-one **(17)**

An oven-dried 50mL round bottom flask was prepared with a magnetic stirring bar, a rubber septum cover, and a nitrogen inlet. 4-hydroxycoumarin (**24**) (172 mg, 1.06 mmol) and 2 mL of anhydrous N,N-dimethylformamide (DMF) were added to the round bottom flask, which was again evacuated and purged with nitrogen. The solution was stirred and cooled to 0ºC in a salt-ice bath. Sodium hydride (51 mg of 60% mineral oil suspension, 2.1 mmol) was added to the flask, at which point H_2 gas began to form. The solution was then stirred at 0ºC for 30 minutes, under nitrogen gas. Geranyl bromide (400 µL, 1.29 g/mL, 2.3 mmol) in 1 mL of anhydrous DMF was cooled to 0ºC and added drop-wise to the flask through the rubber septum using a syringe. The reaction mixture was left to stir under nitrogen and warm back to room temperature overnight. The desired product was obtained by preparative thin layer chromatography using a solvent system of 70% hexanes and 30% ethyl acetate (rf = 0.56). The purified product was verified by NMR spectroscopy (^{1}H-NMR, ^{13}C-NMR) and high-resolution mass spectrometry (HRMS). ^{1}H-NMR (300 MHz, $(CD_3)_2CO$): ∂ 1.61 – 2.16 (17H), 4.85 – 4.87 (s, 2H), 5.12 (m, 1H), 5.60 (d, 1H), 5.78 (s, 1H); 7.29 – 7.35 (m, 2H), 7.60 – 7.66 (m, 1H), 7.81-7.84 (m, 1H). ^{13}C-NMR (75 MHz, $(CD_3)_2CO$): ∂ 16.47, 17.71, 23.86, 25.81, 27.37, 40.49, 105.28, 116.87, 118.54, 122.66, 124.20, 125.11, 129.64, 131.65, 131.88, 132.00, 136.44, 153.55, 163.98. HRMS (EI) Calcd. for $C_{19}H_{22}O_3$: 298.1569; found: 298.1570.

Synthesis of 4-(((2E,6E)-3,7,11-trimethyldodeca-2,6,10-trien-1-yl)oxy)-2H-chromen-2-one **(18)**

An oven-dried 25mL round bottom flask was prepared with a magnetic stirring bar, a rubber septum cover, and a nitrogen inlet. 4-hydroxycoumarin (**24**) (168 mg, 1.03 mmol) and 1 mL of anhydrous N,N-dimethylformamide (DMF) were added to the round bottom flask, which was again evacuated and purged with nitrogen. The solution was stirred and cooled to 0ºC in a salt-ice bath. Sodium hydride (60 mg of 60% mineral oil suspension, 2.5 mmol) was added to the flask, at which point H_2 gas began to form. The solution was then stirred at 0ºC for 30 minutes, under nitrogen gas. Farnesyl bromide (541 µL, 1.05 g/mL, 1.9 mmol) in 1 mL of anhydrous DMF was cooled to 0ºC and added drop-wise to the flask through the rubber septum using a syringe. The reaction mixture was left to stir under nitrogen and warm back to room temperature overnight. The desired product was obtained by preparative thin layer chromatography using a solvent system of 70% hexanes and 30% ethyl acetate (rf = 0.57). The purified product was verified by NMR spectroscopy (^{1}H-NMR, ^{13}C-NMR) and high-resolution mass spectrometry (HRMS). ^{1}H-NMR (300 MHz, $(CD_3)_2CO$): ∂ 1.54 – 2.17 (26H), 4.85 – 4.87 (s, 2H), 5.15 (d, 2H), 5.60 (1H), 5.78 (s, 1H), 7.30 – 7.35 (m, 2H), 7.60 – 7.66 (1H), 7.81-7.84 (m, 1H)**;** ^{13}C-NMR (75 MHz, $(CD_3)_2CO$): ∂ 16.13, 16.44, 16.78, 17.73, 23.31, 25.85, 26.77, 27.40, 28.32, 37.89, 39.87, 40.12, 40.42, 43.29, 67.20, 91.50, 111.28, 116.71, 118.11, 118.76, 123.86, 124.16, 124.48, 124.66, 125.10, 125.68, 129.13, 131.64, 133.25, 136.03, 143.76, 146.88, 154.32, 162.28, 165.82. HRMS (EI) Calcd. for $C_{24}H_{30}O_3$: 366.2195; found: 366.2196.

Synthesis of 4,7-bis((3-methylbut-2-en-1-yl)oxy)-2*H*-chromen-2-one (KE-1-79, **19**)
An oven-dried 50mL round bottom flask was prepared with a magnetic stirring bar, a rubber septum cover, and a nitrogen inlet. 4,7-dihydroxycoumarin (**Z**) (180 mg, 1.01 mmol) and 1 mL of anhydrous N,N-dimethylformamide (DMF) were added to the round bottom flask, which was again evacuated and purged with nitrogen. The solution was stirred and cooled to 0ºC in a salt-ice bath. Sodium hydride (80 mg of 60% mineral oil suspension, 2 mmol) was added to the flask, at which point H_2 gas began to form. The solution was then stirred at 0ºC for 30 minutes, under nitrogen gas. 3,3-dimethyl bromide (462 µL, 1.29 g/mL, 2.0 mmol) in 1 mL of anhydrous DMF was cooled to 0ºC and added drop-wise to the flask through the rubber septum using a syringe. The reaction mixture was left to stir under nitrogen and warm back to room temperature, overnight. Reaction products were purified using preparative thin layer chromatography. The desired product was not formed.

Synthesis of 7-(((E*)*-3*,*7-dimethylocta-2,6-dien-1-yl)oxy)-4-(((Z*)*-3*,*7-dimethylocta-2,6-dien-1-yl)oxy)-2*H*-chromen-2-one (KE-1-83, **20**)

An oven-dried 50mL round bottom flask was prepared with a magnetic stirring bar, a rubber septum cover, and a nitrogen inlet. 4,7-dihydroxycoumarin (**Z**) (182 mg, 1.02 mmol) and 1 mL of anhydrous N,N-dimethylformamide (DMF) were added to the round bottom flask, which was again evacuated and purged with nitrogen. The solution was stirred and cooled to 0ºC in a salt-ice bath. Sodium hydride (80 mg of 60% mineral oil suspension, 2.0 mmol) was added to the flask, at which point H_2 gas began to form. The solution was then stirred at 0ºC for 30 minutes, under nitrogen gas. Geranyl bromide (673 μL, 1.29 g/mL, 2.0 mmol) in 1 mL of anhydrous DMF was cooled to 0ºC and added drop-wise to the flask through the rubber septum using a syringe. The reaction mixture was left to stir under nitrogen and warm back to room temperature overnight. Reaction products were purified using preparative thin layer chromatography. The desired product was not formed.

Synthesis of 7-(((2*E*,6*E*)-3,7,11-trimethyldodeca-2,6,10-trien-1-yl)oxy)-4-(((2*Z*,6*E*)-3,7,11-trimethyldodeca-2,6,10-trien-1-yl)oxy)-2*H*-chromen-2-one (KE-1-84, **21**)

An oven-dried 50mL round bottom flask was prepared with a magnetic stirring bar, a rubber septum cover, and a nitrogen inlet. 4,7-dihydroxycoumarin (**Z**) (190 mg, 1.06 mmol) and 1 mL of anhydrous N,N-dimethylformamide (DMF) were added to the round bottom flask, which was again evacuated and purged with nitrogen. The solution was stirred and cooled to 0ºC in a salt-ice bath. Sodium hydride (80 mg of 60% mineral oil suspension, 2 mmol) was added to the flask, at which point H_2 gas began to form. The solution was then stirred at 0ºC for 30 minutes, under nitrogen gas. Farnesyl bromide (1.08 mL, 1.05 g/mL, 2.0 mmol) in 1 mL of anhydrous DMF was cooled to 0ºC and added drop-wise to the flask through the rubber septum using a syringe. The reaction mixture was left to stir under nitrogen and warm back to room temperature overnight. Reaction products were purified using preparative thin layer chromatography. The desired product was not formed.

*Synthesis of 6-((3,7-dimethyloctyl)oxy)-2H-chromen-2-one (***22,** *CC-I-3)*:*
An oven dried 50mL round bottom flask was prepared with a magnetic stirring bar, a rubber septum cover, and a nitrogen inlet. 6-hydroxycoumarin (114 mg, 0.7 mmol) and 4 mL of anhydrous N,N-dimethylformamide (DMF) were added to the round bottom flask. The solution was stirred and cooled to 0ºC in a salt-ice bath. Sodium hydride (28 mg of 60% mineral oil suspension, 0.7 mmol) was added to the flask at which point the solution turned color from yellow to orange. The solution was kept stirring at 0ºC for 30 minutes. 1-Bromo-3,7-dimethyloctane (344.4 µL, 1.66 mmol) in 1 mL of DMF was cooled to 0ºC and added drop-wise to the flask through the rubber septum using a syringe. The reaction mixture was left stirring under nitrogen to warm back to room temperature over 14 hours. The desired product was obtained through preparative thin layer chromatography using a 7:3 Hexanes:Ethyl acetate solvent system. The purified product was verified by NMR spectroscopy (^{1}H-NMR, ^{12}C-NMR) and high-resolution mass spectrometry (HRMS). ^{1}H-NMR (300 MHz, CD_3COCD_3): ∂ 0.95-1.86 (19H), 4.08 (t, 2H), 6.40 (d, 1H, J=9Hz), 7.17 (m, 2H), 7.27 (s, 1H), 7.92 (d, 1H, J=9Hz); ^{13}C-NMR (75 Hz, CD_3COCD_3): ∂ 19.91, 22.87, 22.97, 25.13, 25.37, 36.60, 37.92, 39.93, 67.54, 111.97, 117.58, 118.47, 120.28, 120.56, 129.10, 144.35, 149.19, 156.44, 160.77. HRMS (EI) Calcd. for $C_{19}H_{26}O_3$: 302.18820; found: 302.18871.

*Synthesis of (R)-6-((3,7-dimethyloct-6-en-1-yl)oxy)-2H-chromen-2-one (***23,** *CC-I-19)*:*
An oven dried 50mL round bottom flask was prepared with a magnetic stirring bar, a rubber septum cover, and a nitrogen inlet. 6-hydroxycoumarin (114 mg, 0.7 mmol) and 4 mL of anhydrous N,N-dimethylformamide (DMF) were added to the round bottom flask. The solution was stirred and cooled to 0ºC in a salt-ice bath. Sodium hydride (28 mg of 60% mineral oil suspension, 0.7 mmol) was added to the flask. The solution was kept stirring at 0ºC for 30 minutes. 8-Bromo-2,6-dimethyl-2-octene-(R)-(-)-citronellyl bromide (327.8 µL, 1.66 mmol) in 1 mL of DMF was cooled to 0ºC and added drop-wise to the flask through the rubber septum using a syringe. The reaction mixture was left stirring under nitrogen to warm back to room temperature over 14 hours. The desired product was obtained through preparative thin layer chromatography using a 7:3 Hexanes:Ethyl acetate solvent system. The purified product was verified by NMR spectroscopy (^{1}H-NMR, ^{12}C-NMR) and high-resolution mass spectrometry (HRMS). ^{1}H-NMR (300 MHz, CD_3COCD_3): ∂ 1.30-2.07 (16H), 4.09 (t, 2H), 5.11 (m, 1H), 6.40 (d, 1H, J=6Hz), 7.22 (m, 3H), 7.92 (d, 1H, J=6Hz); ^{13}C-NMR (75 Hz, CD_3COCD_3): ∂ 17.72, 19.84, 25.86, 26.35, 36.51, 38.53, 67.37, 112.37, 117.33, 118.43, 120.24, 120.52, 125.66, 129.07, 131.51, 144.29, 149.16, 156.40, 160.72. HRMS (EI) Calcd. for $C_{19}H_{24}O_3$: 300.1725; found: 300.1726.

*Synthesis of (S)-6-((3,7-dimethyloct-6-en-1-yl)oxy)-2H-chromen-2-one (***24,** *CC-I-23)*:*
An oven dried 50mL round bottom flask was prepared with a magnetic stirring bar, a rubber septum cover, and a nitrogen inlet. 6-hydroxycoumarin (86 mg, 0.5 mmol) and 4 mL of anhydrous N,N-dimethylformamide (DMF) were added to the round bottom flask. The solution was stirred and cooled to 0ºC in a salt-ice bath. Sodium hydride (21.2 mg of 60% mineral oil suspension, 0.5 mmol) was added to the flask**.** The solution was kept stirring at 0ºC for 30 minutes. 8-Bromo-2,6-dimethyl-2-octene-(S)-(+)-citronellyl bromide (327.8 µL, 1.66 mmol) in 1 mL of DMF was cooled to 0ºC and added drop-wise to the flask through the rubber septum using a syringe. The reaction mixture was left stirring under nitrogen to warm back to room temperature over 14 hours. The desired product was obtained through preparative thin layer chromatography using a 7:3 Hexanes:Ethyl acetate solvent system. The purified product was verified by NMR spectroscopy (^{1}H-NMR, ^{12}C-NMR) and high-resolution mass spectrometry (HRMS). ^{1}H-NMR (300 MHz, CD_3COCD_3): ∂ 1.30-2.07 (16H), 4.09 (t, 2H), 5.11 (m, 1H), 6.40 (d, 1H, J=9Hz), 7.22 (m, 3H), 7.92 (d, 1H, J=9Hz); ^{13}C-NMR (75 Hz, CD_3COCD_3): ∂ 17.72, 19.81, 26.19, 26.36, 37.40, 39.69, 67.52, 111.52, 117.32, 118.46, 120.26, 120.54, 125.62, 129.08, 131.54, 143.98, 149.18, 156.42, 160.75. HRMS (EI) Calcd. for $C_{19}H_{24}O_3$: 300.1725; found: 300.1723.

*Compound was synthesized by Carrico-Moniz lab member, Christine Chun, 15'.

Viability Assay

All cell lines were cultured in complete DMEM (Sigma Aldrich) at 37°C in 5% CO_2. In the interest of consistency, cell passage number was recorded for all cell lines and only cells within P39-P48 were used in viability assays. On the first day of the viability assay, cell density was determined and cells were seeded into a 96-well clear bottom plate at a density of $2.3x10^4$ cells per well. Cells were left to incubate for 24 hours. Meanwhile, fully characterized compounds were vacuum-dried for a minimum of two hours and dissolved in dimethyl sulfoxide (DMSO). On the second day of the assay, the DMSO/compound mixture was then diluted in nutrient-rich or nutrient-deprived media (media recipe can be found in Appendix XII) to a concentration of 1.1 mM in 5.5% DMSO. The cells were then washed with 1x phosphate buffer solution (PBS). Next, the compound solution was added to each well and further diluted to a final compound concentration of 100, 50, 25, 12.5 or 6.25 μM. Each concentration/media condition was run in triplicate. Cells were incubated with coumarin derivatives for 24 hours. Following the incubation period, the cells were, again, washed with 1x PBS. In preparation for the colorimetric viability assay, cells were incubated with complete DMEM (Sigma) and WST-8 kit (Dojindo). After three hours, the absorbance of each well at 450 nm was determined. Cell viability was calculated, per well, using the following equation:

$(Abs_{450} - Blank_2)/(Blank_1-Blank_2)$

where $Blank_1$ corresponds to absorbance at 450 nm in wells containing cells, media, WST-8 kit and 5.5% DMSO and $Blank_2$ refers to the absorbance at 450 nm in wells containing only the media and WST-8 kit.

Index of Appendices

** indicates that compound was synthesized and characterized by fellow lab member, Christine Chun '15*

Appendix I

H^1-NMR in acetone-d6 of

4-((3-methylbut-2-en-1-yl)oxy)-2H-chromen-2-one **(**KE-1-39-2**, 16)**

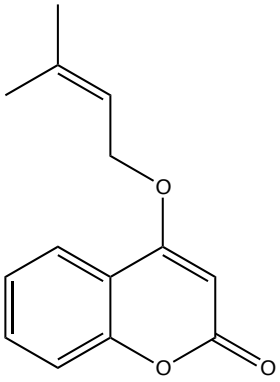

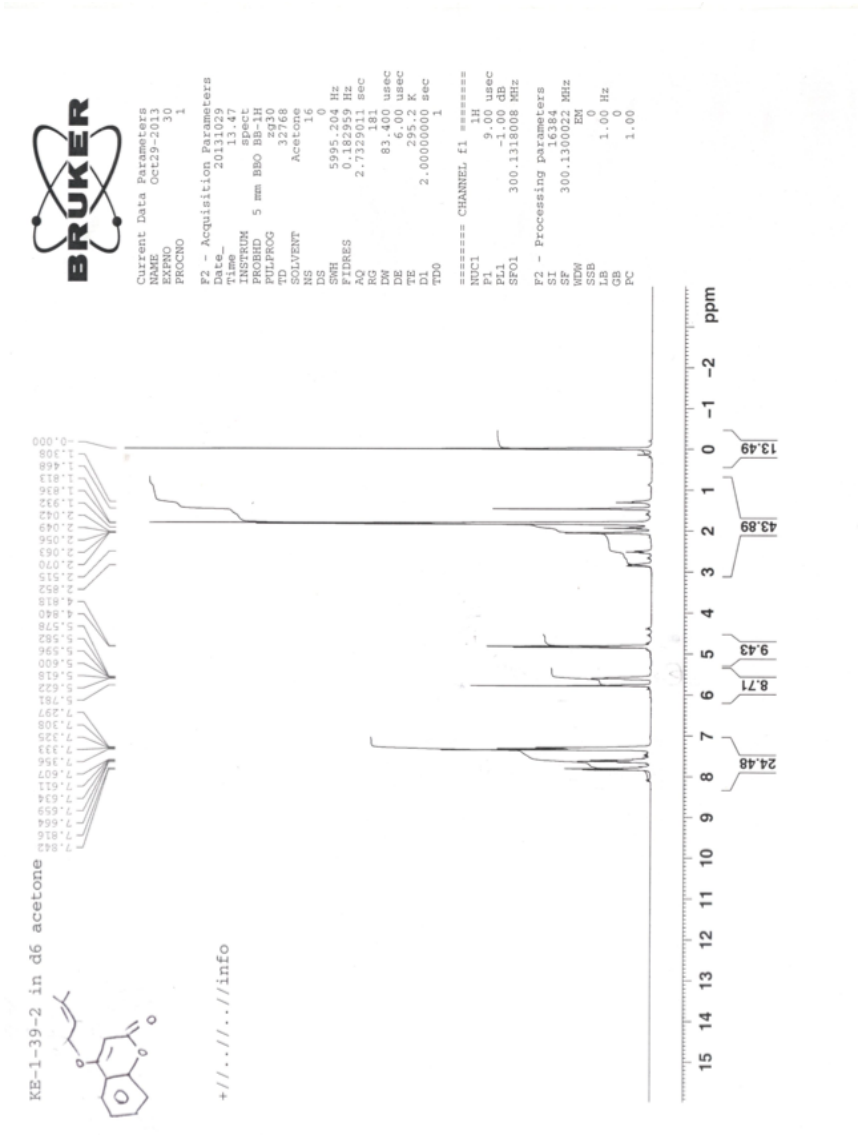

Appendix II

C^{13}-NMR in acetone-d6 of

4-((3-methylbut-2-en-1-yl)oxy)-2H-chromen-2-one **(**KE-1-39-2, **16)**

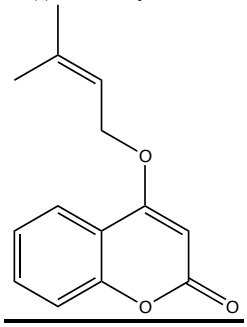

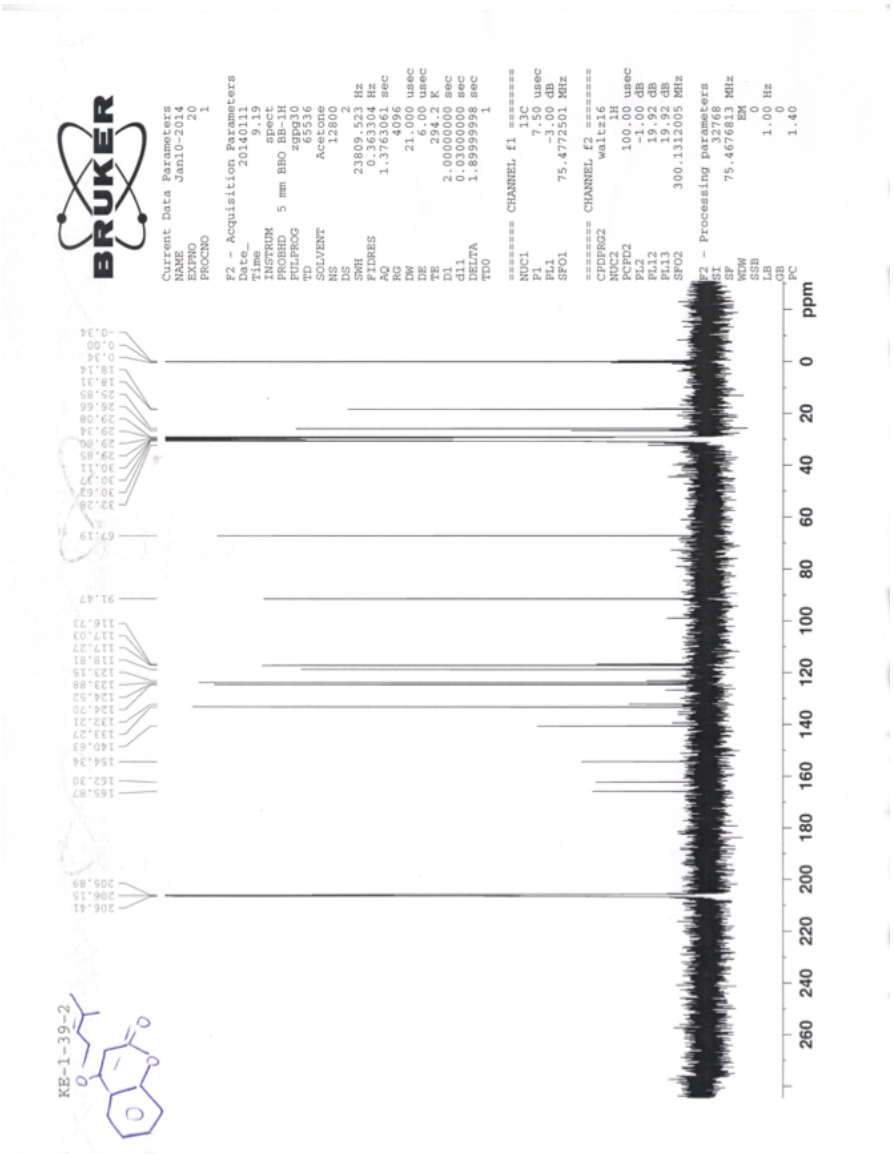

Appendix III

H^1-NMR in acetone-d6 of

(E)-4-((3,7-dimethylocta-2,6-dien-1-yl)oxy)-2H-chromen-2-one **(**KE-1-59-2**, 17)**

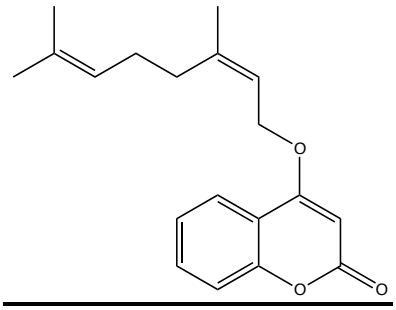

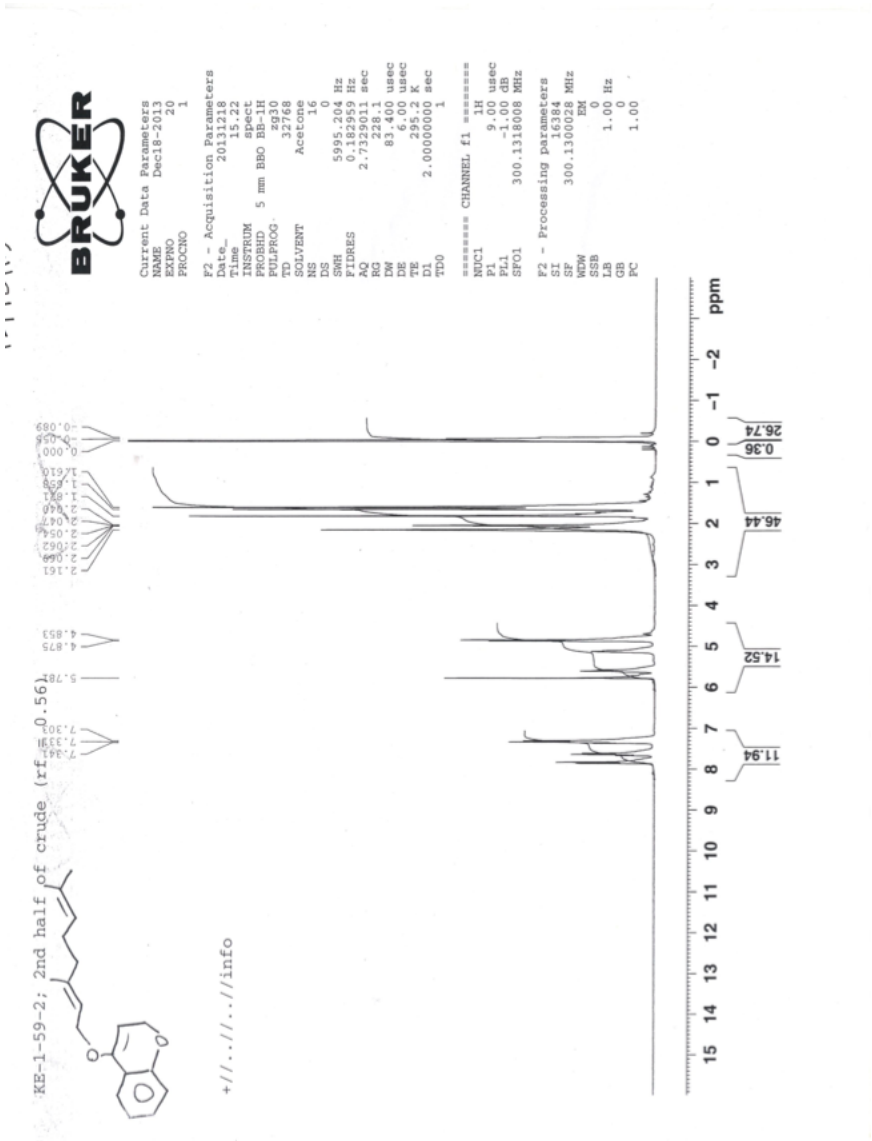

Appendix IV

C^{13}-NMR in acetone-d6 of

(E)-4-((3,7-dimethylocta-2,6-dien-1-yl)oxy)-2H-chromen-2-one **(**KE-1-59-2**, 17)**

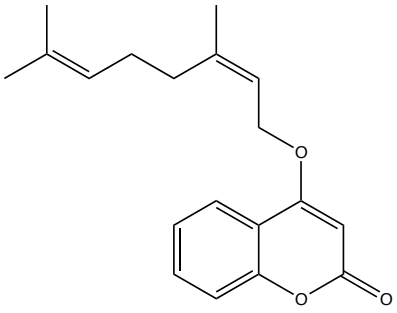

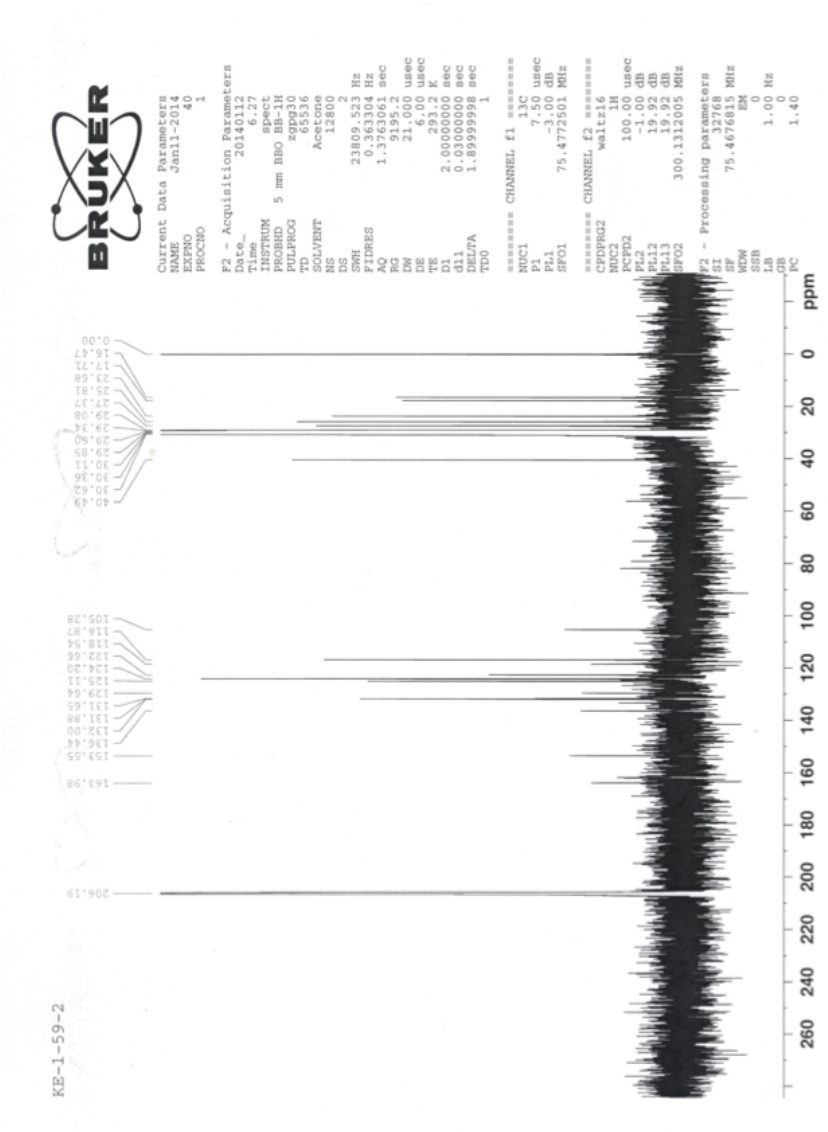

Appendix V

H^1-NMR in acetone-d6 of *4-(((2E,6E)-3,7,11-trimethyldodeca-2,6,10-trien-1-yl)oxy)-2H-chromen-2-one* **(**KE-1-75-3**, 18)**

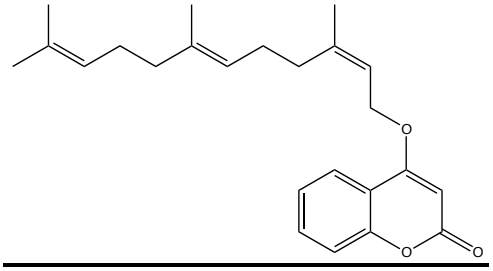

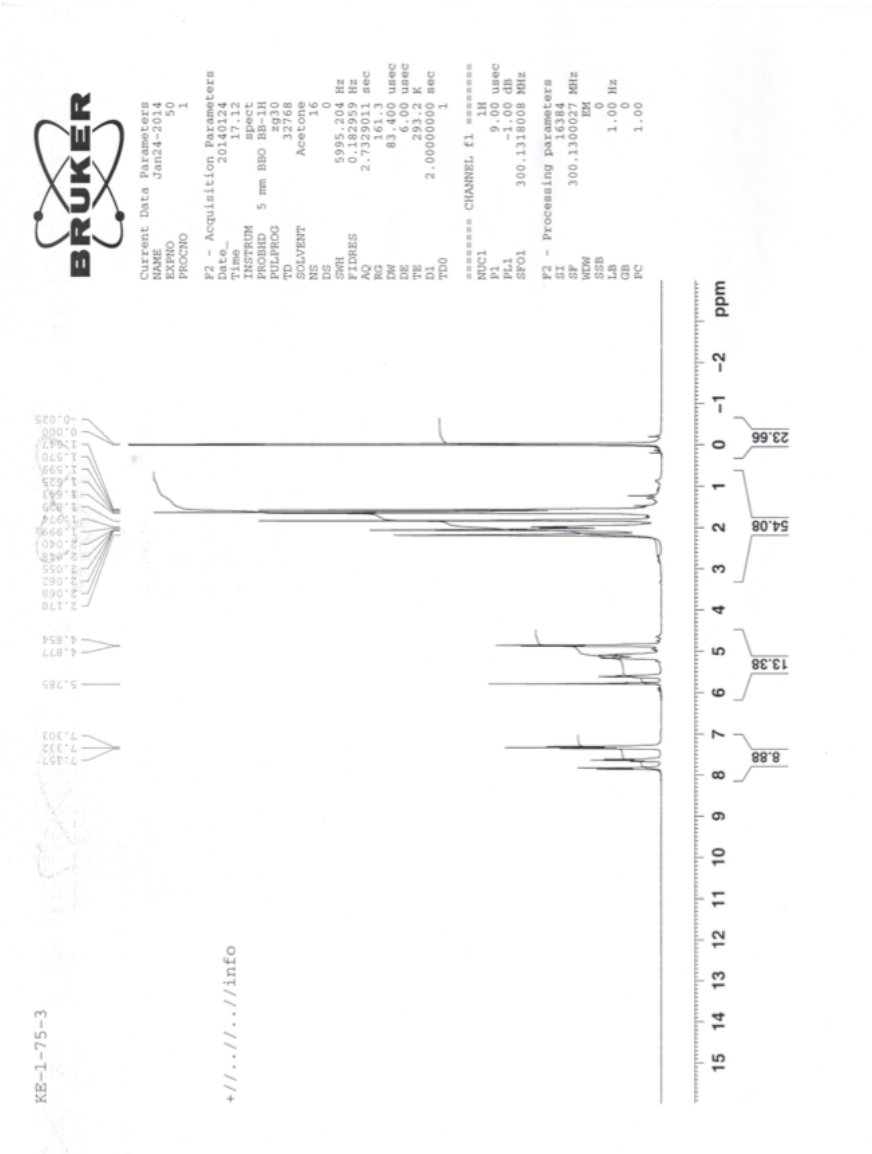

Appendix VI

C^{13}-NMR in acetone-d6 of *4-(((2E,6E)-3,7,11-trimethyldodeca-2,6,10-trien-1-yl)oxy)-2H-chromen-2-one* **(**KE-1-75-3, **18)**

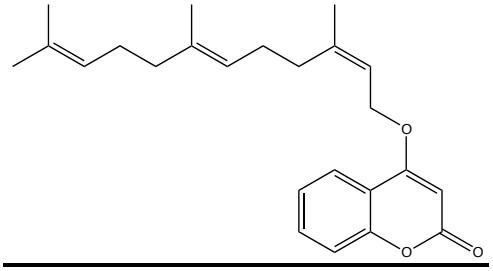

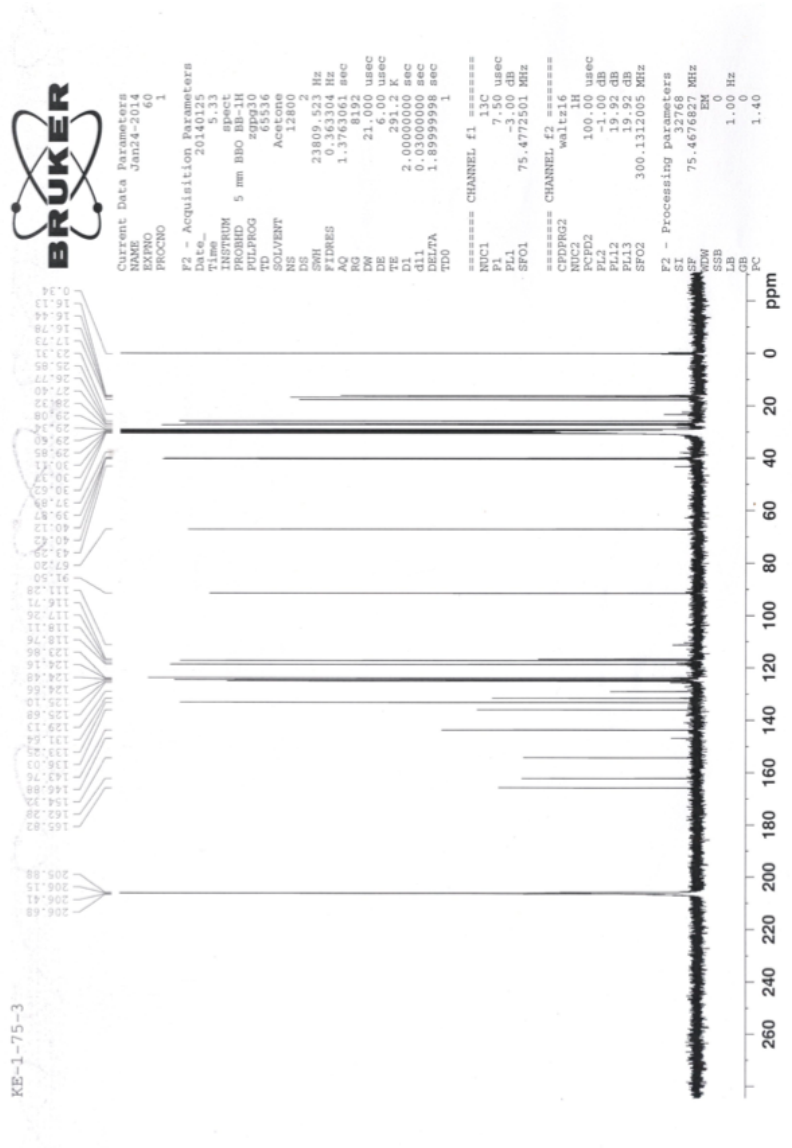

Appendix VII

H^1-NMR in acetone-d6 of KE-1-79-2 (**19**)

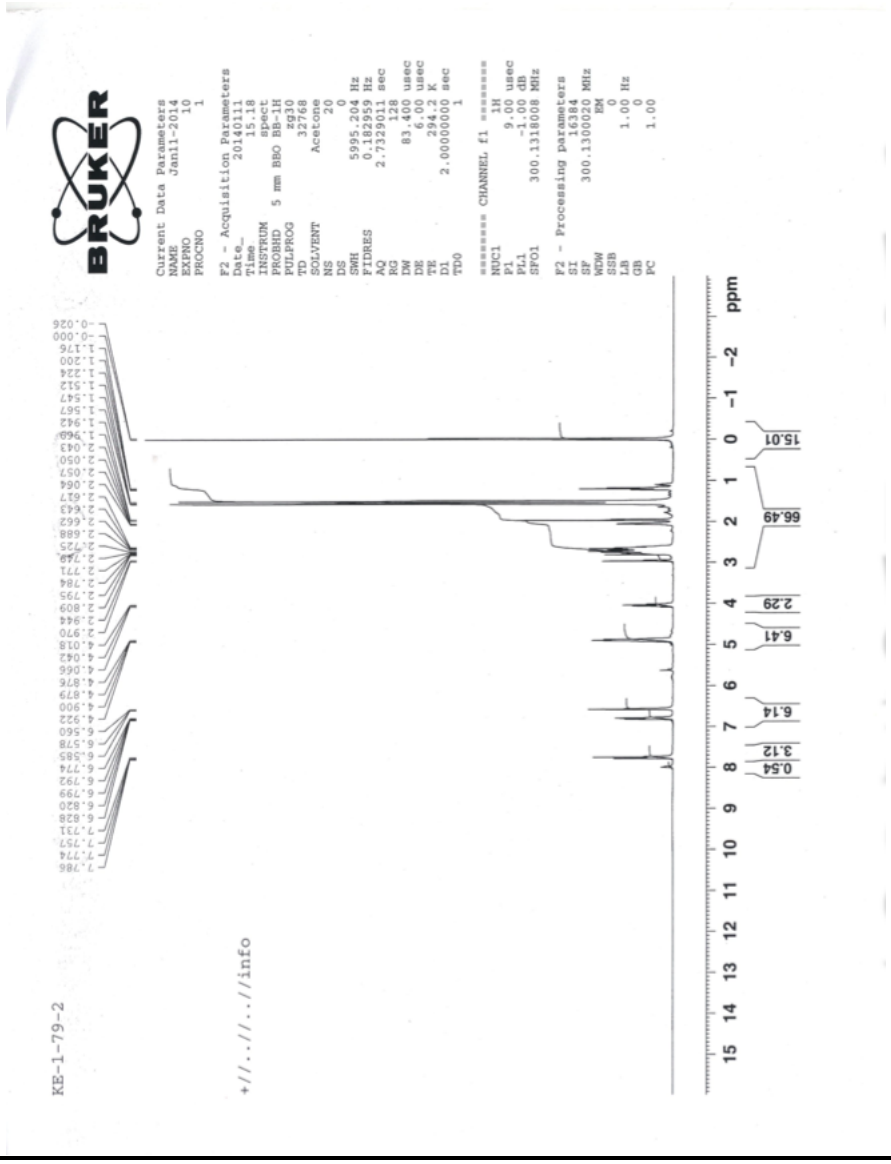

Appendix VIII

H^1-NMR in acetone-d6 of KE-1-79-3 **(19)**

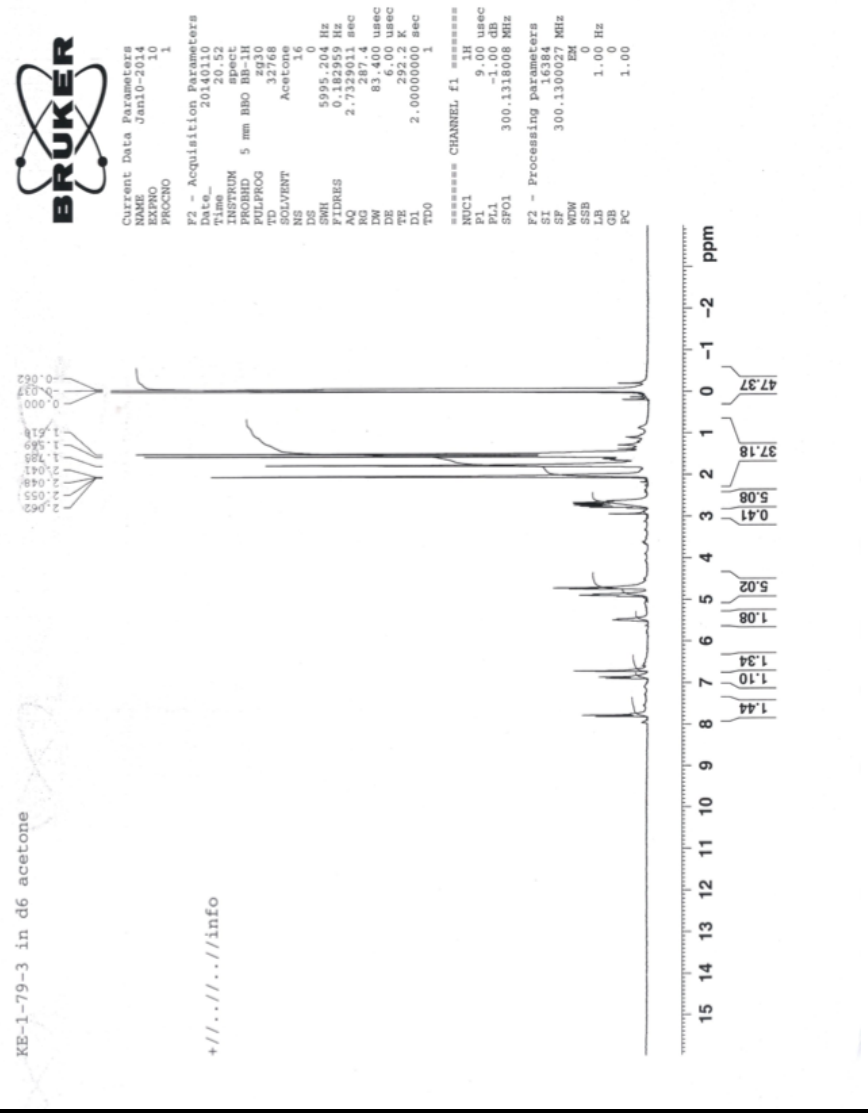

Appendix IX

HRMS (Q-tof) of

4-((3-methylbut-2-en-1-yl)oxy)-2H-chromen-2-one (KE-1-39-2**, 16)**

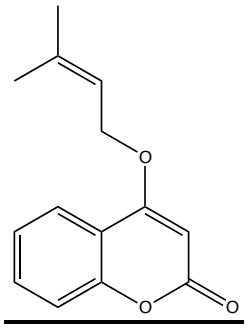

Elemental Composition Report **Page 1**

Single Mass Analysis

Tolerance = 10.0 PPM / DBE: min = -1.5, max = 600.0

Element prediction: Off

Number of isotope peaks used for i-FIT = 3

Monoisotopic Mass, Even Electron Ions

48 formula(e) evaluated with 1 results within limits (all results (up to 1000) for each mass)

Elements Used:

C: 0-125 H: 0-250 O: 0-7 Na: 0-1

Dora Carrico-Moniz, KE-1-39-2 University of Illnois, SCS, Mass Spectrometry Lab Q-tof UE521

Qtof_50951 32 (2.357) AM (Cen,3, 80.00, Ar,15000.0,716.46,0.70); Sm (SG, 2x3.00); Cm (30:35) 2: TOF MS ES+ 1.63e+003

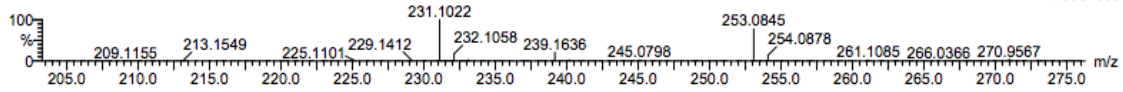

Minimum:				-1.5		
Maximum:		5.0	10.0	600.0		
Mass	Calc. Mass	mDa	PPM	DBE	i-FIT	Formula
231.1022	231.1021	0.1	0.4	7.5	0.7	C14 H15 O3

Appendix X
HRMS (Q-tof) of
4-((3-methylbut-2-en-1-yl)oxy)-2H-chromen-2-one **(**KE-1-39-2**, 16)**

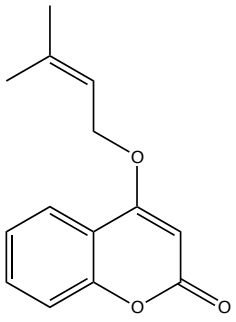

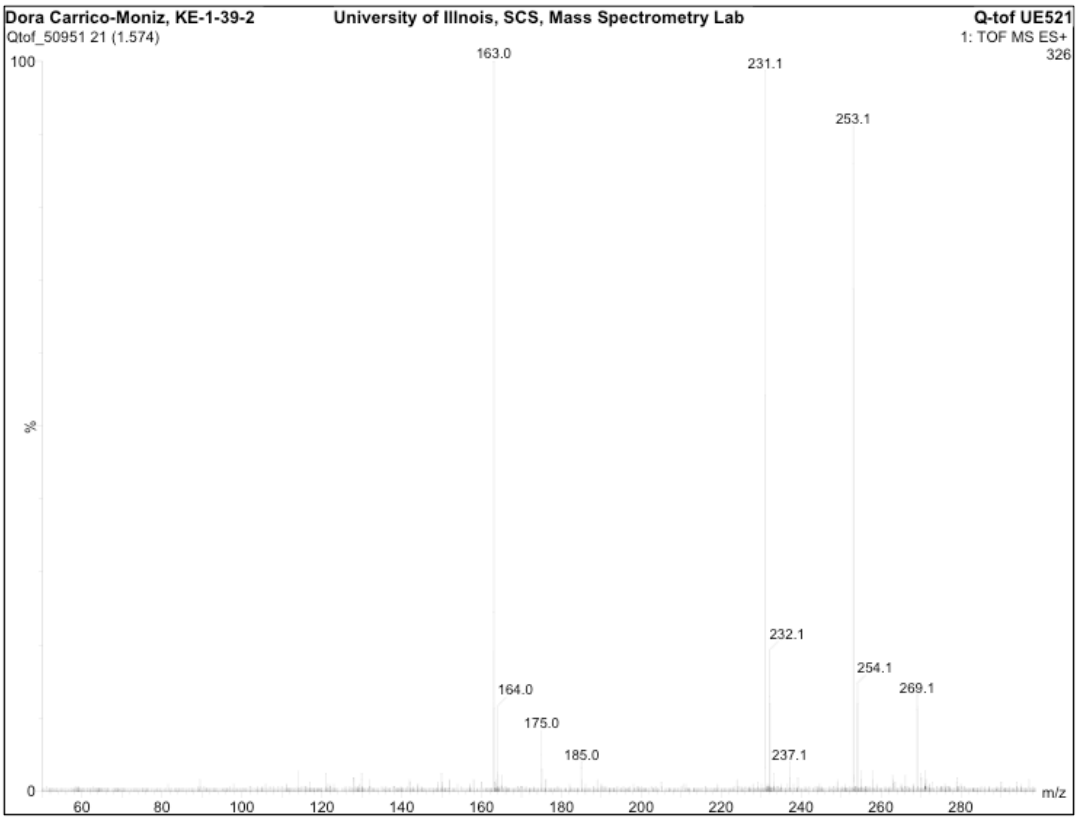

Appendix XI
HRMS (EI) of
(E)-4-((3,7-dimethylocta-2,6-dien-1-yl)oxy)-2H-chromen-2-one (KE-1-59-2**, 17)**

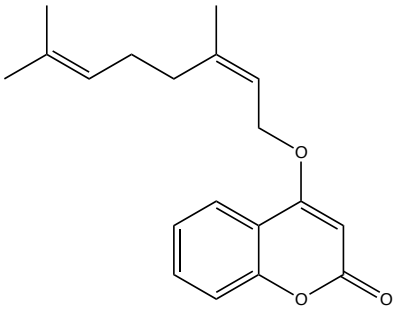

Elemental Composition Report **Page 1**

Single Mass Analysis
Tolerance = 5.0 mDa / DBE: min = -1.5, max = 50.0
Element prediction: Off

Monoisotopic Mass, Odd and Even Electron Ions
12 formula(e) evaluated with 1 results within limits (up to 50 best isotopic matches for each mass)
Elements Used:
C: 0-50 H: 0-100 O: 2-4
Dora Carrico-Moniz, KE-1-59-2
KE-1-59-2 1618 (10.149)

TOF MS EI+
1.05e+002

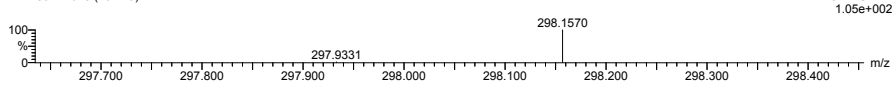

Minimum:				-1.5		
Maximum:		5.0	10.0	50.0		
Mass	Calc. Mass	mDa	PPM	DBE	i-FIT	Formula
298.1570	298.1569	0.1	0.3	9.0	5546065.0	C19 H22 O3

Appendix XII
HRMS (EI) of
(E)-4-((3,7-dimethylocta-2,6-dien-1-yl)oxy)-2H-chromen-2-one (KE-1-59-2**, 17)**

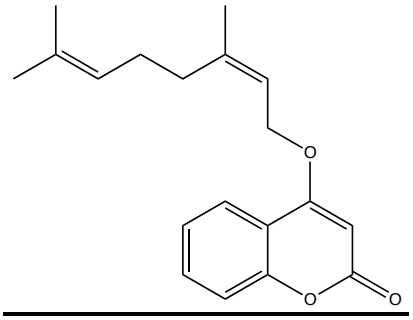

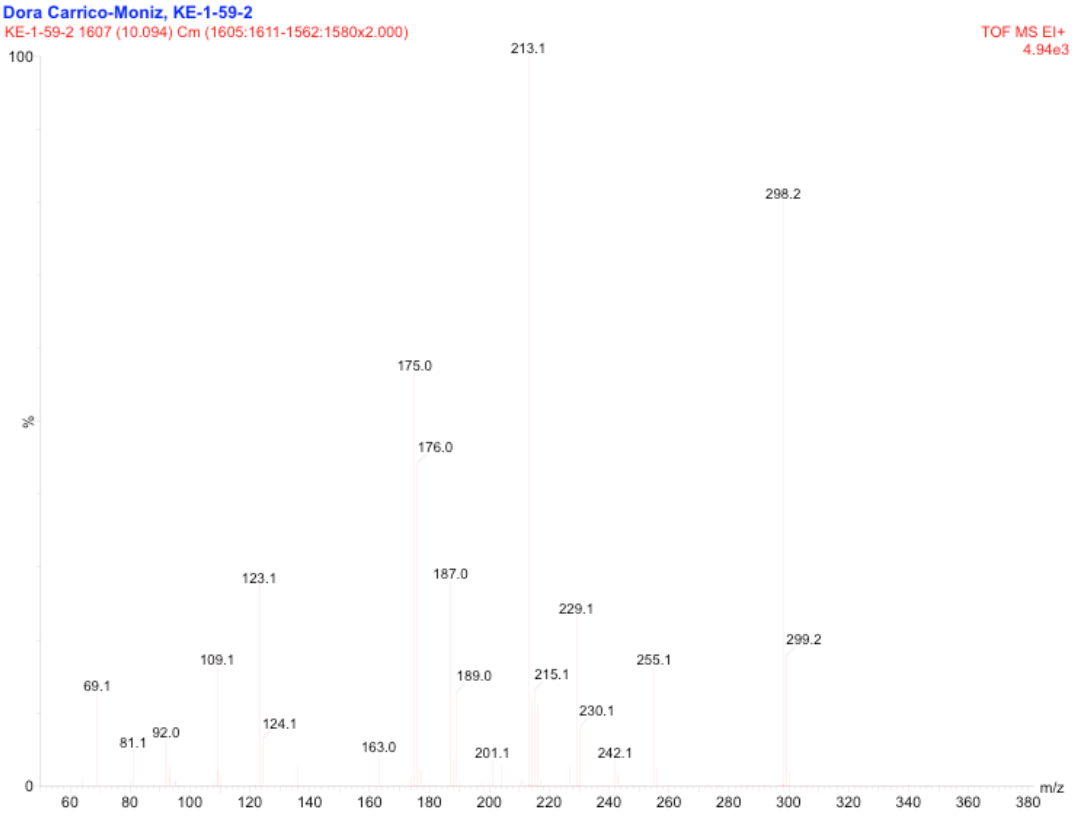

Appendix XIII
HRMS (EI) of
4-(((2E,6E)-3,7,11-trimethyldodeca-2,6,10-trien-1-yl)oxy)-2H-chromen-2-one **(**KE-1-75-3**, 18)**

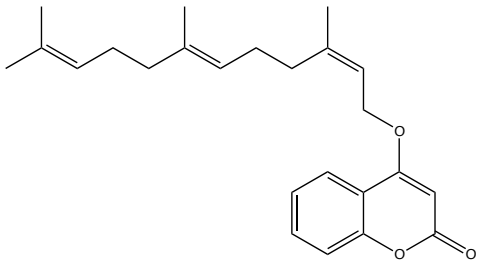

Elemental Composition Report **Page 1**

Single Mass Analysis
Tolerance = 5.0 mDa / DBE: min = -1.5, max = 50.0
Element prediction: Off

Monoisotopic Mass, Odd and Even Electron Ions
15 formula(e) evaluated with 1 results within limits (up to 50 best isotopic matches for each mass)
Elements Used:
C: 0-50 H: 0-100 O: 2-4
Dora Carrico-Moniz, KE-1-75-3
KE-1-75-3a 2488 (14.499)

TOF MS EI+
1.91e+003

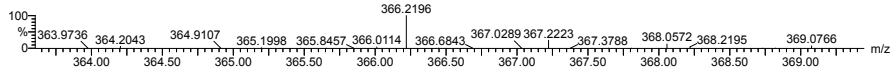

Minimum:				-1.5		
Maximum:		5.0	10.0	50.0		
Mass	Calc. Mass	mDa	PPM	DBE	i-FIT	Formula
366.2196	366.2195	0.1	0.3	10.0	3.1	C24 H30 O3

Appendix XIV
HRMS (EI) of
4-(((2E,6E)-3,7,11-trimethyldodeca-2,6,10-trien-1-yl)oxy)-2H-chromen-2-one **(**KE-1-75-3**, 18)**

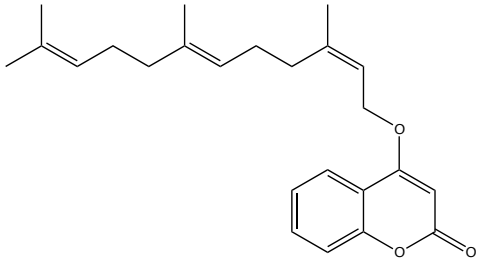

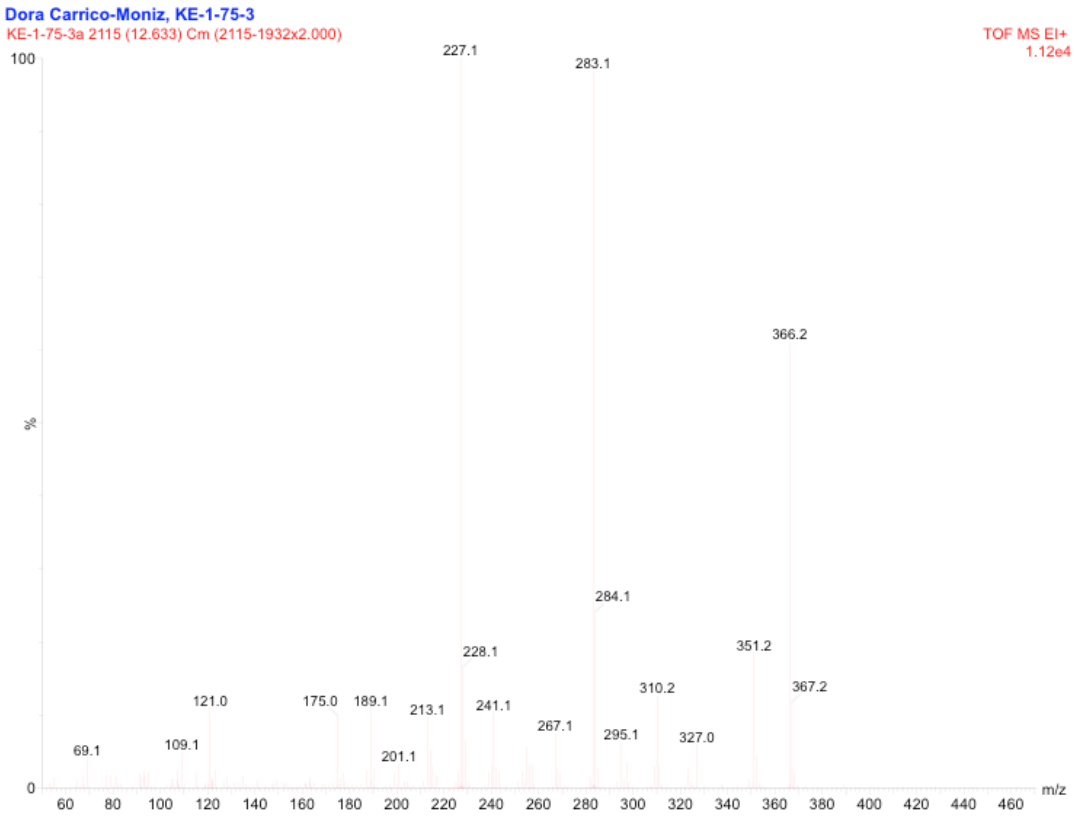

Appendix XV

H^1-NMR in acetone-d6 of *6-((3,7-dimethyloctyl)oxy)-2H-chromen-2-one (***22,** *CC-I-3)**

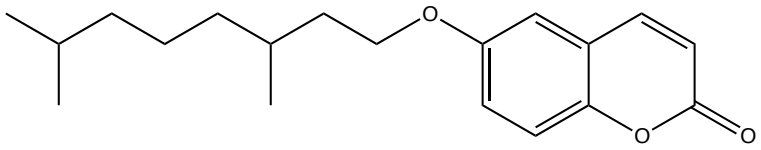

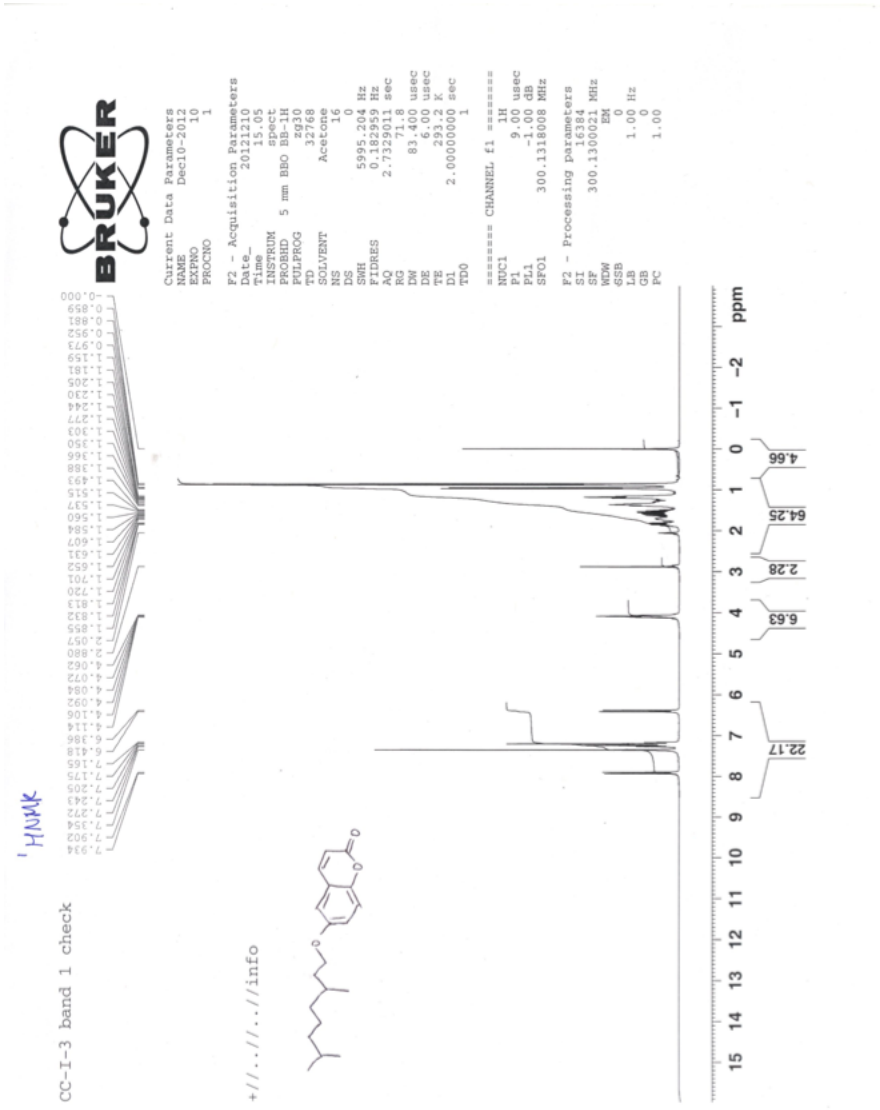

Appendix XVI

C^{13}-NMR in acetone-d6 of *6-((3,7-dimethyloctyl)oxy)-2H-chromen-2-one (***22,** *CC-I-3)**

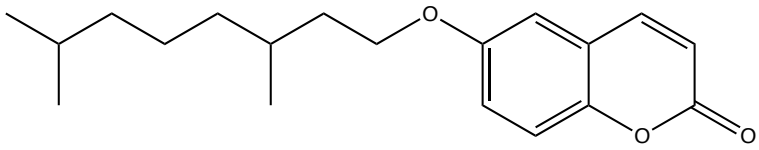

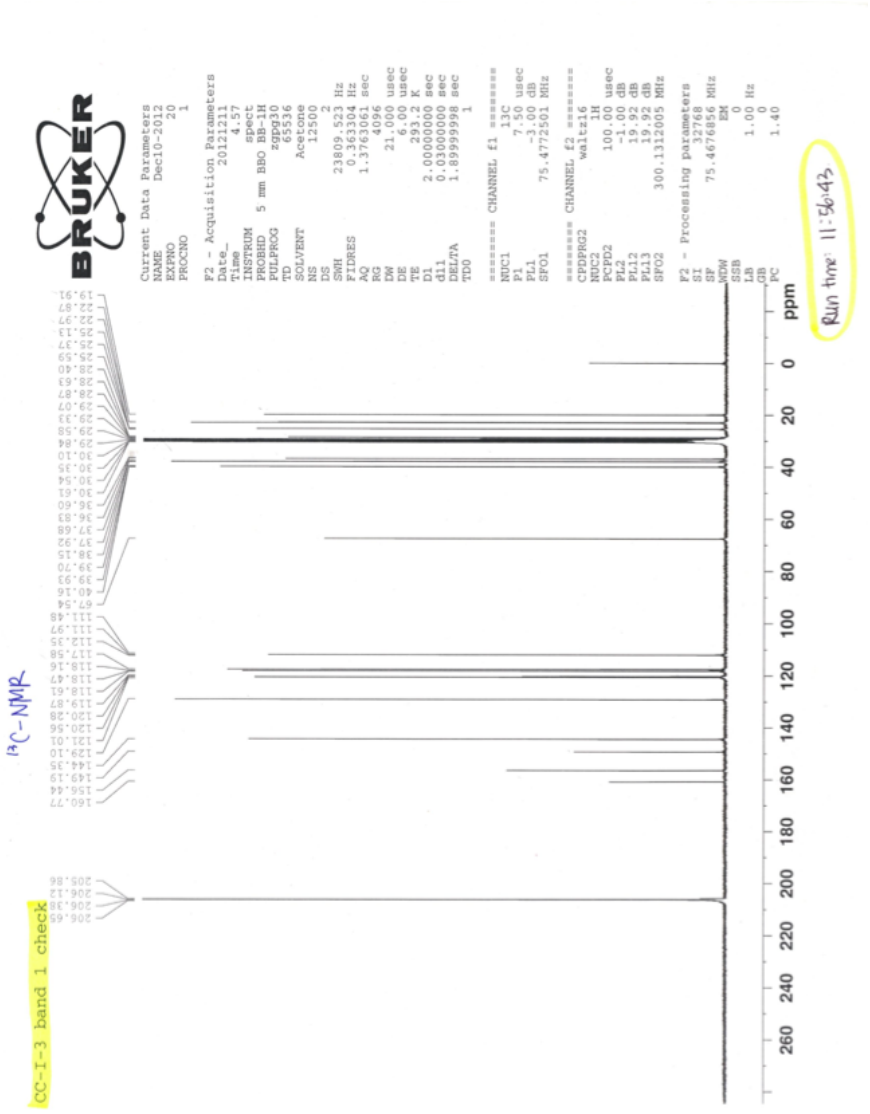

Appendix XVII

HRMS (EI) for *6-((3,7-dimethyloctyl)oxy)-2H-chromen-2-one (***22,** *CC-I-3)**

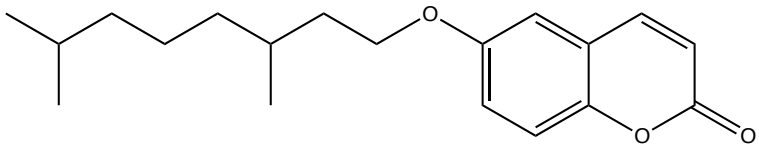

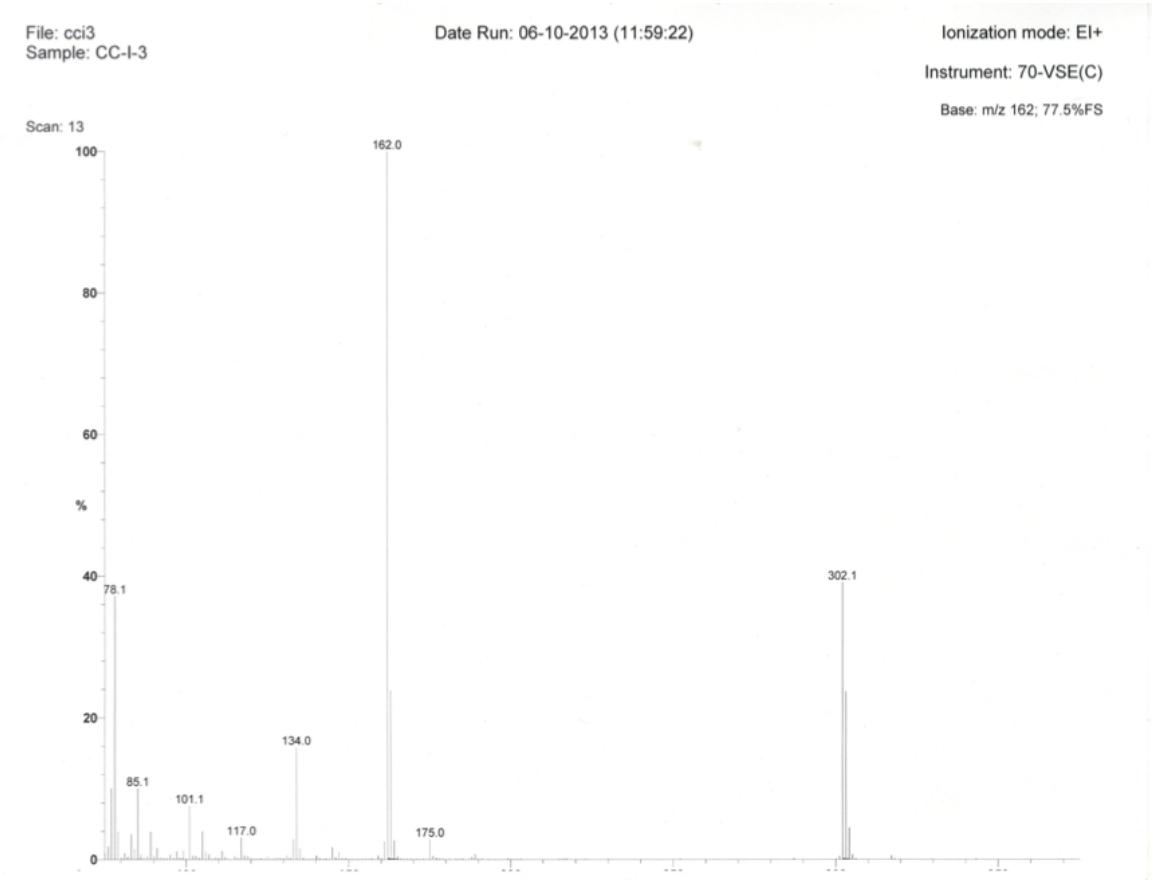

Appendix XVIII

HRMS (EI) for *6-((3,7-dimethyloctyl)oxy)-2H-chromen-2-one (***22,** *CC-I-3)**

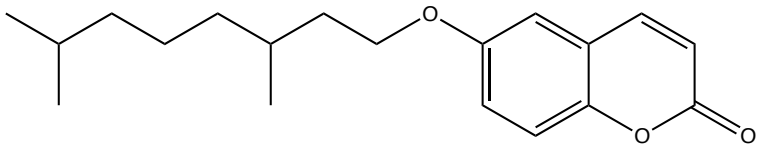

File: cci3
Sample: CC-I-3

Date Run: 06-10-2013 (11:59:22)

Ionization mode: EI+

Instrument: 70-VSE(C)

Base: m/z 162; 77.5%FS

Scan: 13

Threshold: 2% of Base

Displayed TIC: 682725

Mass	%Base	Mass	%Base	Mass	%Base	Mass	%Base	Mass	%Base	Mass	%Base	Mass	%Base	Mass	%Base	Mass	%Base	Mass	%Base
77.1	10.0	79.1	3.9	85.1	10.0	101.1	7.6	117.0	3.1	134.0	15.8	162.0	100.0	164.0	2.7	302.1	39.1	304.1	4.4
78.1	37.2	83.1	3.6	89.1	3.9	105.0	4.0	133.0	2.9	161.0	2.5	163.0	23.8	175.0	2.9	303.1	23.7	304.2	4.6

File: cci3hr
Sample: CC-I-3

Date Run: 06-10-2013 (18:00:43)

Ionization mode: EI+

Instrument: 70-VSE(C)

Base: m/z 302; 30.7%FS

Scan: 35

Selected Isotopes : C H O_{0-3}

Error Limit : 5 ppm

Unsaturation Limits : -.5 to 30

Measured Mass	*% Base*	*Formula*	*Calculated Mass*	*Error*	*Unsaturation*
302.18871	100.0%	$C_{19}H_{26}O_3$	302.18820	1.7	7.0

Appendix XIX

H^1-NMR in acetone-d6 of

*(R)-6-((3,7-dimethyloct-6-en-1-yl)oxy)-2H-chromen-2-one (***23,** *CC-I-19)**

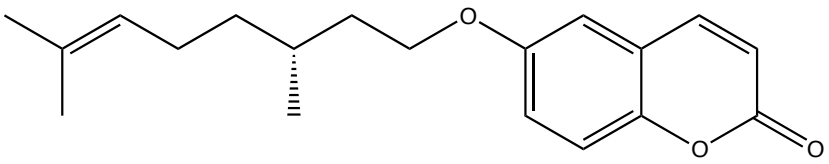

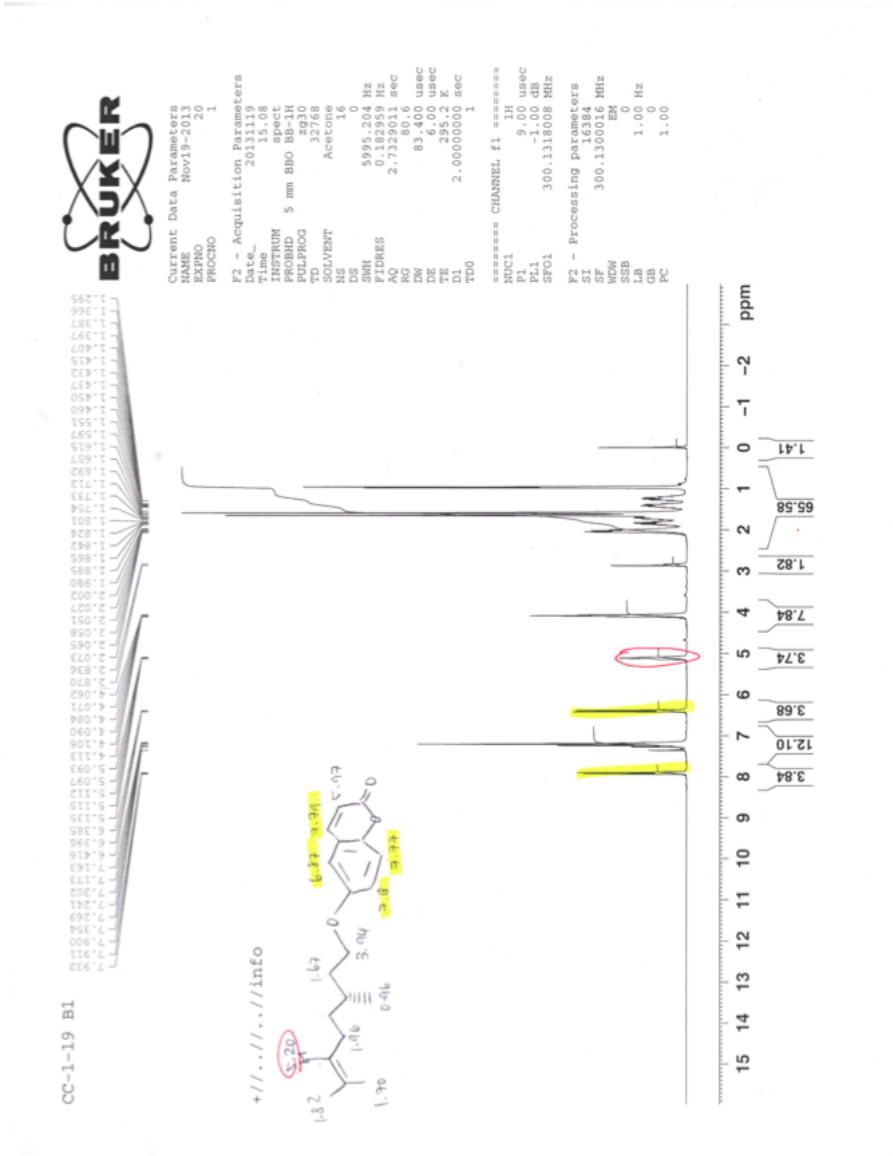

Appendix XX

C^{13}-NMR in acetone-d6 of

*(R)-6-((3,7-dimethyloct-6-en-1-yl)oxy)-2H-chromen-2-one (***23,** *CC-I-19)**

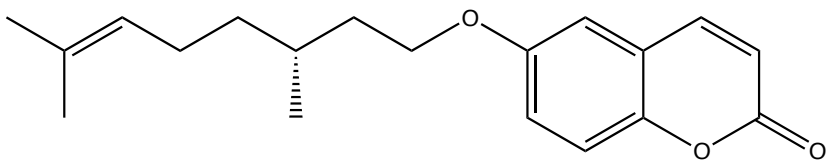

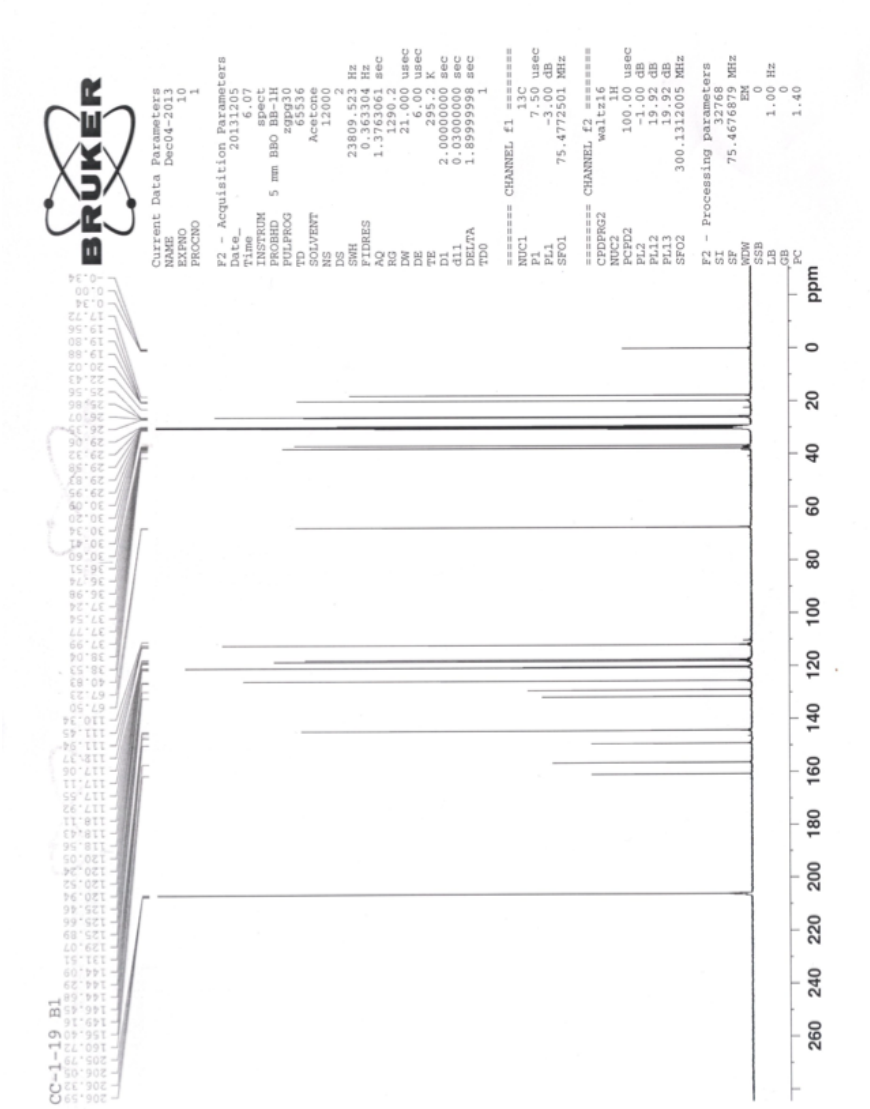

Appendix XXI

HRMS (EI) for

*(R)-6-((3,7-dimethyloct-6-en-1-yl)oxy)-2H-chromen-2-one (***23,** *CC-I-19)**

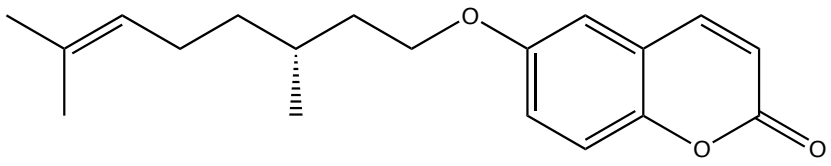

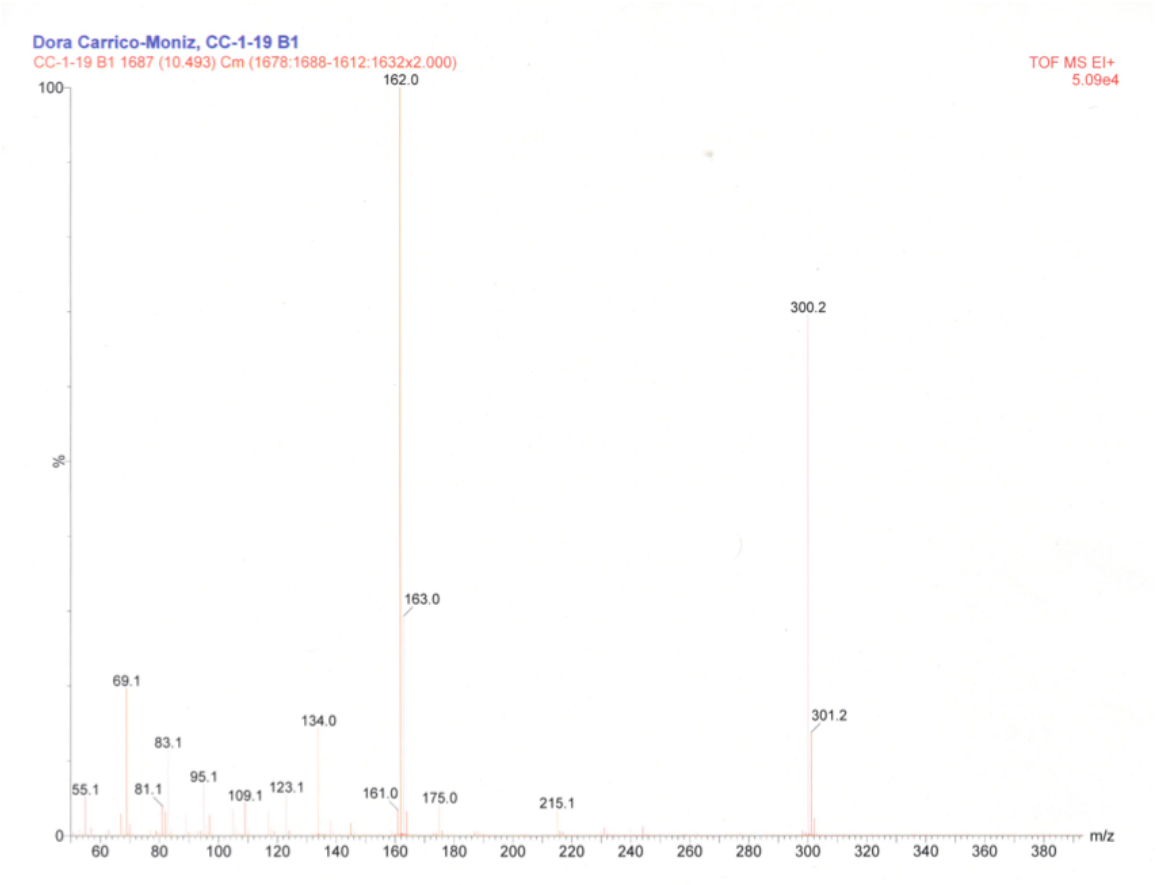

Appendix XXII

HRMS (EI) for

*(R)-6-((3,7-dimethyloct-6-en-1-yl)oxy)-2H-chromen-2-one (***23,** *CC-I-19)**

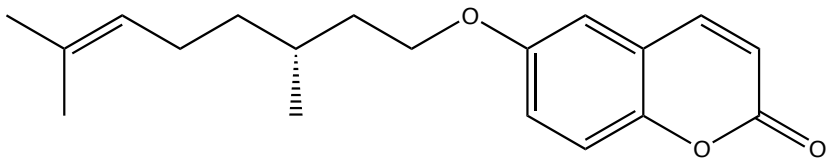

Elemental Composition Report **Page 1**

Single Mass Analysis
Tolerance = 5.0 mDa / DBE: min = -1.5, max = 50.0
Element prediction: Off

Monoisotopic Mass, Odd and Even Electron Ions
12 formula(e) evaluated with 1 results within limits (up to 50 best isotopic matches for each mass)
Elements Used:
C: 0-50 H: 0-100 O: 2-4
Dora Carrico-Moniz, CC-1-19 B1
CC-1-19 B1 1681 (10.464)

TOF MS EI+
3.39e+003

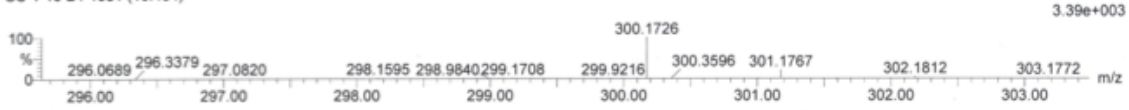

Minimum:				-1.5		
Maximum:		5.0	10.0	50.0		
Mass	Calc. Mass	mDa	PPM	DBE	i-FIT	Formula
300.1726	300.1725	0.1	0.3	8.0	3.3	C19 H24 O3

Appendix XXIII

H^1-NMR in acetone-d6 of

*(S)-6-((3,7-dimethyloct-6-en-1-yl)oxy)-2H-chromen-2-one (***24,** *CC-I-23)*:*

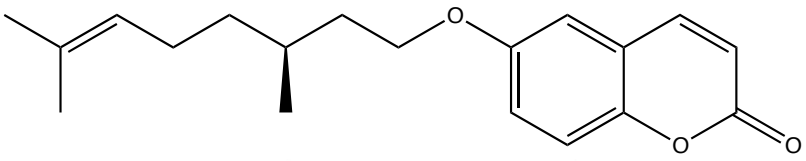

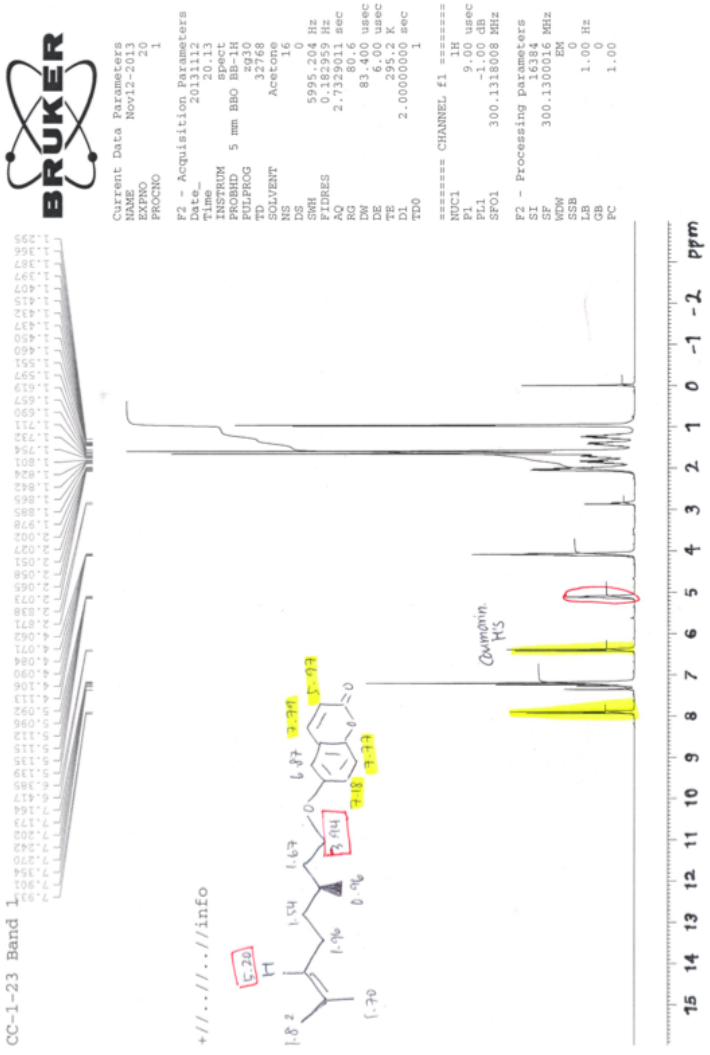

Appendix XXIV

C^{13}-NMR in acetone-d6 of
*(S)-6-((3,7-dimethyloct-6-en-1-yl)oxy)-2H-chromen-2-one (***24,** *CC-I-23)*:*

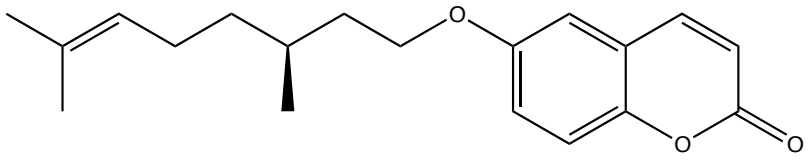

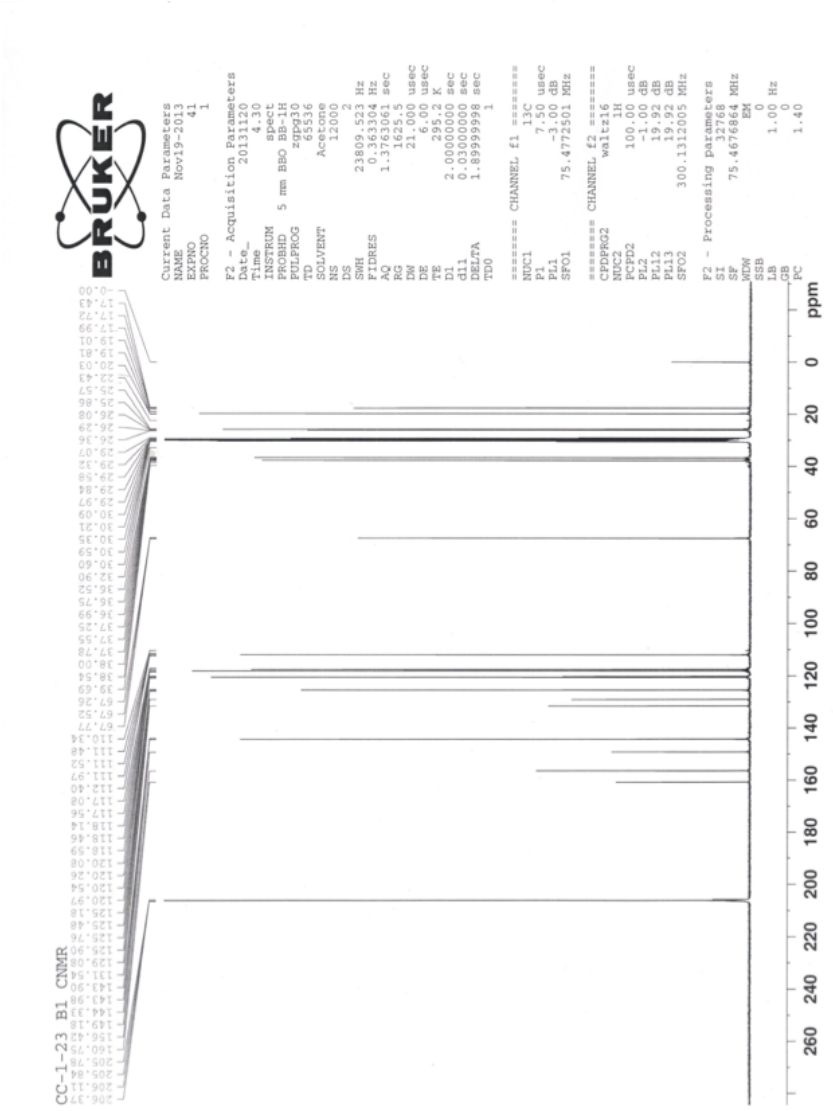

Appendix XXV

HRMS (EI) of

*(S)-6-((3,7-dimethyloct-6-en-1-yl)oxy)-2H-chromen-2-one (***24,** *CC-I-23)*:*

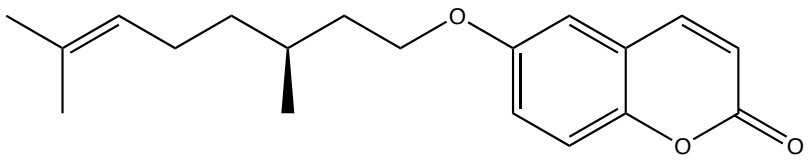

Appendix XXVI

HRMS (EI) for
*(S)-6-((3,7-dimethyloct-6-en-1-yl)oxy)-2H-chromen-2-one (***24,** *CC-I-23)*:*

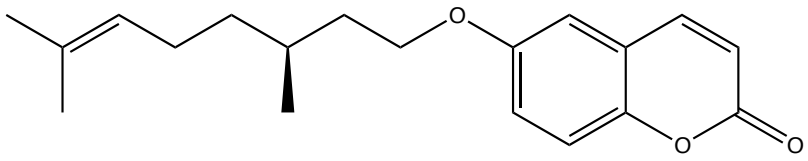

Elemental Composition Report **Page 1**

Single Mass Analysis
Tolerance = 5.0 mDa / DBE: min = -1.5, max = 50.0
Element prediction: Off

Monoisotopic Mass, Odd and Even Electron Ions
12 formula(e) evaluated with 1 results within limits (up to 50 best isotopic matches for each mass)
Elements Used:
C: 0-50 H: 0-100 O: 2-4
Dora Carrico-Moniz, CC-1-23 B1
CC-1-23 B1 1662 (10.368)

TOF MS EI+
3.05e+003

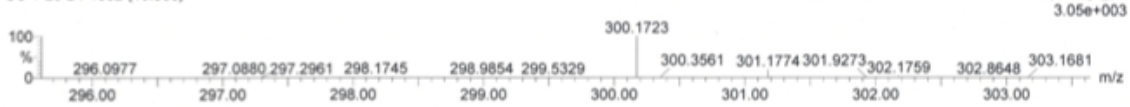

Minimum:				-1.5		
Maximum:		5.0	10.0	50.0		
Mass	Calc. Mass	mDa	PPM	DBE	i-FIT	Formula
300.1723	300.1725	-0.2	-0.7	8.0	7.5	C19 H24 O3

Appendix XXVII

Preparation of complete DMEM from powder

To prepare complete DMEM, one bottle of Dulbecco Modified Eagle's Minimum Essential Media (Sigma Aldrich) was dissolved in 800 mL of HPLC-purified water. Sodium bicarbonate (49.1 mL) and 100x anti-biotic/anti-fungal solution (10 mL) were then added to the solution and the total volume was brought to 900 mL using HPLC water and adjusted to a pH of 7.4. Half of this mixture, 450 mL, was then combined with 50 mL of heat-inactivated FBS, filtered using a 0.2 μm filtering unit and stored at 4° C.

Appendix XXVIII

Composition of media made from scratch:

- $CaCl_2$ (0.265 mg/mL)
- $FeNO_3$ (0.001 mg/mL)
- KCl: (0.400 mg/mL)
- $MgSO_4$: (0.200 mg/mL)
- NaCl: (6.400 mg/mL)
- $NaHCO_3$ (0.700 mg/mL)
- NaH_2PO: (0.125 mg/mL)
- Phenol red: (0.015 mg/mL)
- HEPES buffer: (5.958 g/L)
- MEM vitamin solution (1%)
- D-glucose (1 g/L)*
- L-glutamine (2 mM)*
- MEM amino acids solution (2%)*
- MEM nonessential amino acids solution (1%)*
- FCS (10%)*

*Indicates components that are absent in the nutrient-deprived media

Media recipes are based off of a previously published study [8]. All components were dissolved in HPLC water, filtered, corrected to a pH of 7.4 at stored at 4°C.

References

1. Raimondi, S., P. Maisonneuve, and A.B. Lowenfels, *Epidemiology of pancreatic cancer: an overview.* Nat Rev Gastroenterol Hepatol, 2009. **6**(12): p. 699-708.
2. Surgery, C.U.D.o. *Cancer of the Pancreas*. 2013 [cited 2013 Dec. 2013].
3. Lohr, J.M., *Medical treatment of pancreatic cancer.* Expert Rev Anticancer Ther, 2007. **7**(4): p. 533-44.
4. Shore, S., et al., *Cancer in the elderly: pancreatic cancer.* Surg Oncol, 2004. **13**(4): p. 201-10.
5. Win, N.N., et al., *Novel anticancer agents, kayeassamins C-I from the flower of Kayea assamica of Myanmar.* Bioorg Med Chem, 2008. **16**(18): p. 8653-60.
6. *Pancreatic Cancer Treatment*. 2013 [cited 2013 January]; Available from: http://www.cancer.gov/cancertopics/pdq/treatment/pancreatic/Patient/page4.
7. Sicard, F., et al., *Targeting miR-21 for the therapy of pancreatic cancer.* Mol Ther, 2013. **21**(5): p. 986-94.
8. Izuishi, K., et al., *Remarkable tolerance of tumor cells to nutrient deprivation: possible new biochemical target for cancer therapy.* Cancer Res, 2000. **60**(21): p. 6201-7.
9. Magolan, J., et al., *Synthesis and Evaluation of Anticancer Natural Product Analogues Based on Angelmarin: Targeting the Tolerance towards Nutrient Deprivation.* Chemmedchem, 2012. **7**(5): p. 766-770.
10. Singh, S.B., *Pharmaceuticals: natural products and natural product models*, in *Natural Products in Chemical Biology*, N. Civjan, Editor. 2012, Wiley Online Library.
11. Goodman, J. and V. Walsh, *The Story of Taxol: Nature and Politics in the Pursuit of an Anti-Cancer Drug*. 2001: Cambridge University Press. 282.
12. Awale, S., et al., *Angelmarin, a novel anti-cancer agent able to eliminate the tolerance of cancer cells to nutrient starvation.* Bioorg Med Chem Lett, 2006. **16**(3): p. 581-3.
13. Lee, C.-L., et al., *Influenza A (H(1)N(1)) Antiviral and Cytotoxic Agents from Ferula assa-foetida.* Journal of natural products U6 - ctx_ver=Z39.88-2004&ctx_enc=info%3Aofi%2Fenc%3AUTF-8&rfr_id=info:sid/summon.serialssolutions.com&rft_val_fmt=info:ofi/fmt:kev:mtx:journal&rft.genre=article&rft.atitle=Influenza+A+%28H%281%29N%281%29%29+Antiviral+and+Cytotoxic+Agents+from+Ferula+assa-foetida&rft.jtitle=Journal+of+natural+products&rft.au=Lee%2C+Chia-Lin&rft.au=Chiang%2C+Lien-Chai&rft.au=Cheng%2C+Li-Hung&rft.au=Liaw%2C+Chih-Chuang&rft.date=2009-09-01&rft.eissn=1520-6025&rft.volume=72&rft.issue=9&rft.spage=1568&rft_id=info:pmid/19691312&rft.externalDocID=19691312&paramdict=en-US U7 - Journal Article U8 - FETCH-pubmed_primary_19691312, 2009. **72**(9): p. 1568.
14. Mahendra, P. and S. Bisht, *Ferula asafoetida: Traditional uses and pharmacological activity.* Pharmacogn Rev, 2012. **6**(12): p. 141-6.
15. Nazari, Z.E. and M. Iranshahi, *Biologically Active Sesquiterpene Coumarins from Ferula Species.* Phytotherapy Research, 2011. **25**(3): p. 315-323.

16. Devji, T., et al., *Pancreatic anticancer activity of a novel geranylgeranylated coumarin derivative.* Bioorg Med Chem Lett, 2011. **21**(19): p. 5770-3.
17. Borges, F., et al., *Simple coumarins and analogues in medicinal chemistry: occurrence, synthesis and biological activity.* Curr Med Chem, 2005. **12**(8): p. 887-916.
18. Peng, X.M., G.L.V. Damu, and C.H. Zhou, *Current Developments of Coumarin Compounds in Medicinal Chemistry.* Current Pharmaceutical Design, 2013. **19**(21): p. 3884-3930.
19. Bubols, G.B., et al., *The antioxidant activity of coumarins and flavonoids.* Mini Rev Med Chem, 2013. **13**(3): p. 318-34.
20. Piazzi, L., et al., *Multi-target-directed coumarin derivatives: hAChE and BACE1 inhibitors as potential anti-Alzheimer compounds.* Bioorg Med Chem Lett., 2008. **18**(1): p. 423-6.
21. Mohammadi, M., et al., *Two new coumarins from the chloroform extract of Angelica urumiensis from Iran.* Chem Pharm Bull (Tokyo), 2010. **58**(4): p. 546-8.
22. Steffensky, M., et al., *Identification of the novobiocin biosynthetic gene cluster of Streptomyces spheroides NCIB 11891.* Antimicrob Agents Chemother, 2000. **44**(5): p. 1214-22.
23. Sardari, S., et al., *Synthesis and antifungal activity of coumarins and angular furanocoumarins.* Bioorg Med Chem, 1999. **7**(9): p. 1933-40.
24. Devji, T.F., *Design and synthesis of novel isoprenyl coumarin derivatives as potential antiviral and anticancer agents*, in *Chemistry Department*. 2011, Wellesley College.
25. Helmenstine, A.M. *Alpha-Tocopherol - Vitamin E (E307) Chemical Structure*. [cited 2014; Available from: http://chemistry.about.com/od/factsstructures/ig/Chemical-Structures---T/Alpha-Tocopherol.htm.
26. Kontogiorgis, C.A., et al., *Coumarin derivatives protection against ROS production in cellular models of Abeta toxicities.* Free Radic Res, 2007. **41**(10): p. 1168-80.
27. Anand, P., B. Singh, and N. Singh, *A review on coumarins as acetylcholinesterase inhibitors for Alzheimer's disease.* Bioorganic & Medicinal Chemistry, 2012. **20**(3): p. 1175-1180.
28. Lopez-Gonzalez, J.S., et al., *Apoptosis and cell cycle disturbances induced by coumarin and 7-hydroxycoumarin on human lung carcinoma cell lines.* Lung Cancer, 2004. **43**(3): p. 275-83.
29. Ma, Y.M., et al., *Novel microtubule-targeted agent 6-chloro-4-(methoxyphenyl) coumarin induces G(2)-M arrest and apoptosis in HeLa cells.* Acta Pharmacologica Sinica, 2012. **33**(3): p. 407-417.
30. Cohen, A.J., *Critical review of the toxicology of coumarin with special reference to interspecies differences in metabolism and hepatotoxic response and their significance to man.* Food Cosmet. Toxicol., 1979. **17**(3): p. 277-89.
31. Lake, B.G., *Coumarin metabolism, toxicity and carcinogenicity: relevance for human risk assessment.* Food Chem Toxicol, 1999. **37**(4): p. 423-53.

32. Marcu, M.G., T.W. Schulte, and L. Neckers, *Novobiocin and related coumarins and depletion of heat shock protein 90-dependent signaling proteins.* J Natl Cancer Inst, 2000. **92**(3): p. 242-8.
33. Venugopala, K.N., V. Rashmi, and B. Odhav, *Review on Natural Coumarin Lead Compounds for Their Pharmacological Activity.* BioMed Research International, 2013. **2013**.